applied sciences

MDPI

*Article*

# Establishment of Localized Utilization Parameters for Numerical Simulation Analysis Applied to Deep Excavations

**Chien-Yi Wu [1] and Chia-Feng Hsu [2,*]**

[1] Kenkul Corporation Company, New Taipei City 23444, Taiwan; wucy@niu.edu.tw
[2] Department of Civil Engineering, ChienKuo Technology University, Changhua City 500020, Taiwan
* Correspondence: chiafeng1013@gmail.com; Tel.: +886-958786134

**Abstract:** The aim of this study was to apply deep excavation behavior prediction models in the geotechnical field to establish localized soil parameters for gravel layers. Common software tools, including PLAXIS and SoilWorks, were used extensively. Monitoring data from deep excavation cases related to gravel layers in the Xindian area of Taiwan were collected. In the background analysis, the deformation of the retaining walls was used instead of parameters typically used in deep excavation analysis. This was performed to provide the ideal range recommendations for the input parameters when conducting a numerical simulation analysis of the Xindian District stratum or similar strata. The assessment results show that when setting the fifth layer of gravel to *SPT-N* = 100, PLAXIS suggested a soil elastic modulus range of 7840 N to 9800 N per square meter (kN/m$^2$), while SoilWorks recommended a range of 2450 N to 3430 N per square meter (kN/m$^2$). These ranges allow for a reasonable estimation of the maximum wall deformation during the final excavation stage. Based on the research findings, it is recommended that when conducting an excavation analysis in gravel layers in the Xindian area of Taiwan or in similar strata, engineers should refer to the abovementioned recommended ranges when selecting the soil elastic modulus for different software programs. This will enhance the accuracy of the deformation predictions during the final excavation stage.

**Keywords:** deep excavation; gravel layers; localized soil parameters; PLAXIS; SoilWorks



**Citation:** Wu, C.-Y.; Hsu, C.-F. Establishment of Localized Utilization Parameters for Numerical Simulation Analysis Applied to Deep Excavations. *Appl. Sci.* **2023**, *13*, 10127. https://doi.org/10.3390/app131810127

Academic Editor: Mingguang Li

Received: 18 July 2023
Revised: 29 August 2023
Accepted: 6 September 2023
Published: 8 September 2023



## 1. Introduction

The issue of land spatial utilization is a common problem faced with respect to urban areas in Taiwan's development. To effectively compete for space, there is a growing trend of existing buildings undergoing renovations or new buildings being constructed with increased above-ground floors, as well as a shift towards underground development. As a result, building foundations are being dug deeper, and the scale of deep excavation projects is increasing. In recent years, with the continuous updates and changes in analysis software, there has been an increase in the development of programs that combine and utilize drawing software to quickly establish analysis models, set parameters, and perform excavation simulation analyses at various stages, such as GTS and SoilWorks.

Most studies on deep excavations have primarily focused on soft soil layers and sandy layers. Only a limited number of studies in Taiwan have explored the engineering characteristics of gravel layers. Deep excavation engineering is a complex task that involves evaluating the interaction between the soil and structures. The design analysis of deep excavations can make effective use of relevant knowledge and practical experience from the fields of geotechnical and structural engineering. The finite element method employs the concept of continuum mechanics to simulate the behavior of soil and retaining structures during construction, defining the stress–strain relationships and boundary conditions of the soil.

In this study, based on the parameters used for the design analysis of deep excavations in the gravel layer of the Xindian district, the monitoring data collected in this excavation

project were evaluated. Using the PLAXIS 2D and SoilWorks programs as research tools, the aim of this analysis was to explore the behavior of deep excavations in the gravel layers of this district. The findings provide recommendations for the analysis and design of deep excavations in similar gravel-layered settings.

### 1.1. Engineering Properties and Microzonation of Taipei Basin

With regard to the engineering properties and zoning of soils in the Taipei Basin, in 1994, Hung et al. divided the area west of the Tamsui River into four zones based on administrative districts and in situ standard penetration test results [1]. Liu et al. further divided the region west of the Tamsui River, south of the Xindian River, and the Da Han River basin into seven zones based on geological formations [2].

In 1996, Li et al. established a geotechnical database system using approximately 1600 borehole data [3]. They subdivided the engineering geology zoning of Taipei City into 13 zones and extended the zoning to New Taipei City by incorporating approximately 400 borehole data within the New Taipei City area, resulting in a total of seven zones. The proposed engineering geology zoning map for the Taipei Basin was based on this database.

### 1.2. Literature Review on Finite Element Method

The PLAXIS software package is capable of handling various types of geotechnical analysis problems involving plane strain and axisymmetric conditions in two- and three-dimensional space [4]. Analyzing deep excavation projects using the finite element method involves dividing the retaining wall and surrounding soil within the influence range of the excavation depth into multiple meshes. Each mesh is assigned appropriate element types (such as beam elements or bilinear elements) and stress–strain models (such as elastic models, hyperbolic models, or yield surface models) based on their material characteristics and differences. The stress changes and deformations of each element induced by the excavation are then solved using the finite element method [5].

By accurately controlling the construction sequence during deep excavation analysis using the finite element method, it is possible to calculate the displacement of each mesh point within and outside the excavation area. Many domestic researchers have applied the finite element method to successfully obtain the lateral displacements of retaining structures [6–11].

Similarly, some foreign scholars have applied the finite element method to analyze lateral displacements of retaining structures, yielding satisfactory results [12–15]. Recently, Maleki et al. also provided many important conclusions for reference in the field of numerical analysis modeling using the finite element method [16–18].

### 1.3. Soil Elastic Modulus

In numerical analysis, the engineering characteristics of the soil parameters, such as soil cohesion, internal friction angle, and unit weight, can be directly obtained through testing and are commonly used without dispute; however, the elastic modulus of soil cannot be directly determined from tests due to the disturbance caused by soil sampling. Therefore, empirical formulas are often used to estimate the elastic modulus in practical applications.

For clay soils, Bjerrum [19] studied normally consolidated Norwegian clays and proposed the following equation to estimate the elastic modulus of clay:

$$E_s / S_u = (250 \sim 500) \quad (1)$$

where $E_s$ is the elastic modulus and $S_u$ is the undrained shear strength.

For sandy soils, D'Appolonia, Simond, and Bowles proposed methods to estimate the elastic modulus based on the standard penetration test (SPT) $N$-values obtained in the field [20–22].

Bowles [22] provided the empirical relationships shown in Tables A1 and A2 (Appendix A) for estimating the elastic modulus of clay. Li et al. compiled relevant literature and pre-

sented empirical equations for estimating the soil elastic modulus in units of kPa, as shown in Tables 1 and 2 [23].

**Table 1.** Input form of soil layer strength parameters in Case 1.

| Depth (m) | Soil Classification | Use *N* Value | $C'$ (kN/m$^2$) | $\Phi'$ (°) | $\gamma_{unsat}$ (kN/m$^3$) | $\gamma_{sat}$ (kN/m$^3$) | *Es* (kN/m$^2$) | *v* |
|---|---|---|---|---|---|---|---|---|
| 0.0~4.0 | SF, ML, SM | 5 | 0 | 30 | 19.3 | 19.5 | 15,000 N | 0.33 |
| 4.0~15.7 | GW | 40 | 4.9 | 38 | 21.6 | 22.0 | 7840 N–9800 N | 0.28 |
| 15.7~20.3 | GW, SW | 35 | 0 | 38 | 21.1 | 21.4 | 7840 N–9800 N | 0.28 |
| 20.3~24.4 | ML | 16 | 0 | 32 | 19.4 | 19.7 | 100,000 N | 0.32 |
| 24.4~33.0 | GW | 100 | 9.8 | 40 | 22.1 | 22.3 | 7840 N–9800 N | 0.26 |

**Table 2.** Input form of soil layer strength parameters in Case 2.

| Depth (m) | Soil Classification | Use *N* Value | $C'$ (kN/m$^2$) | $\Phi'$ (o) | $\gamma_{unsat}$ (kN/m$^3$) | $\gamma_{sat}$ (kN/m$^3$) | *Es* (kN/m$^2$) | *v* |
|---|---|---|---|---|---|---|---|---|
| 0.0~3.7 | SF, ML | 7 | 0 | 30 | 19.4 | 19.5 | 24,000 N | 0.33 |
| 3.7~16.1 | GW | 40 | 4.9 | 38 | 21.9 | 22.0 | 7840 N–9800 N | 0.28 |
| 16.1~19.5 | GM, SM | 23 | 0 | 34 | 21.1 | 21.4 | 7840 N–9800 N | 0.31 |
| 19.5~24.4 | ML | 13 | 0 | 31 | 19.5 | 19.7 | 100,000 N | 0.33 |
| 24.4~35.5 | GP, GM | 100 | 9.8 | 40 | 22.1 | 22.3 | 7840 N–9800 N | 0.26 |

### *1.4. Literature Review on Sensitivity Analysis of Parameters*

In numerical analyses of foundation excavations, different analysis programs have different theoretical foundations and vary in terms of their input parameters. Although different programs may use different input parameters due to their specific characteristics, the analysis results should exhibit similar trends in retaining-wall deformation.

Hsieh et al. conducted a sensitivity analysis of deep excavation parameters using the RIDO program for representative cases involving sandy and clayey layers [24]. The results show that the $\Phi$ (friction angle) value had a less significant impact on the analysis results, while the Su (undrained shear strength) value was more sensitive. The variation in the horizontal ground reaction coefficient had a lower sensitivity to the maximum bending moment of the retaining wall. When the horizontal ground reaction coefficient was reduced to 1/4 of the reference value, the deformation increased by 60% to 100%, indicating that the $K_h$ value was more sensitive to wall displacement.

Zhang et al. conducted a sensitivity analysis using the RIDO program for a construction site in Taipei [25]. They found that varying the soil friction angle from 0.8 to 1.2 times the original analysis value resulted in an approximately ±4% effect on the retaining wall displacement. Varying the horizontal ground reaction coefficient from 0.5 to 2.0 times the original analysis value resulted in a variation of −25% to 13% in the wall displacement, which was consistent with the findings of Hsieh et al.

Chiu performed a sensitivity analysis using the PLAXIS program, specifically focusing on the effective friction angle and soil elastic modulus [26]. The results show that a smaller $\Phi$ value had a greater impact on the continuous wall bending moment, displacement, and average axial force. The undrained cohesive soil exhibited relatively lower sensitivity to the friction angle. The sensitivity of the average axial force was lower compared to the continuous wall bending moment and displacement. Regarding the sensitivity of the soil elastic modulus, a smaller $E_s$ value had a greater impact on the continuous wall displacement.

### *1.5. Literature Review on Prediction of Maximum Wall Deflection*

Predicting the maximum deflection of a diaphragm wall before construction is a crucial task in building design. It is common to utilize empirical methods and numerical

approaches with sophisticated constitutive models for this purpose [27–29]. Several empirical techniques, expressed through equations or design charts, are available for estimating the maximum wall deflection induced by excavation [30–33].

## 2. Materials and Methods

### 2.1. Research Method and Procedure

The behavior of retaining structure deformation and its impact on the surrounding ground resulting from foundation excavation has been extensively studied both domestically and internationally. The most commonly used 1D retaining wall analysis programs in the engineering industry are the RIDO program developed by Robert Fages Logiciels and the TORSA program developed by the Foundation of Geotechnical Engineering and Technology Research. Additionally, 2D or even 3D numerical analysis software is used for simulation and review, with PLAXIS and FLAC being the most common numerical analysis programs domestically and internationally. In this study, the 2D PLAXIS and SoilWorks programs were selected as research tools. Firstly, a sensitivity analysis was conducted in SoilWorks using the basic case model and variations in the soil parameters adopted in previous studies, and the results were compared with those from the PLAXIS analysis. Furthermore, using the case of gravel layer excavation in the Xindian area, suitable ranges of soil elastic modulus for analysis using PLAXIS and SoilWorks programs were derived.

Based on the explanation above, the workflow for this study is illustrated in Figure 1.

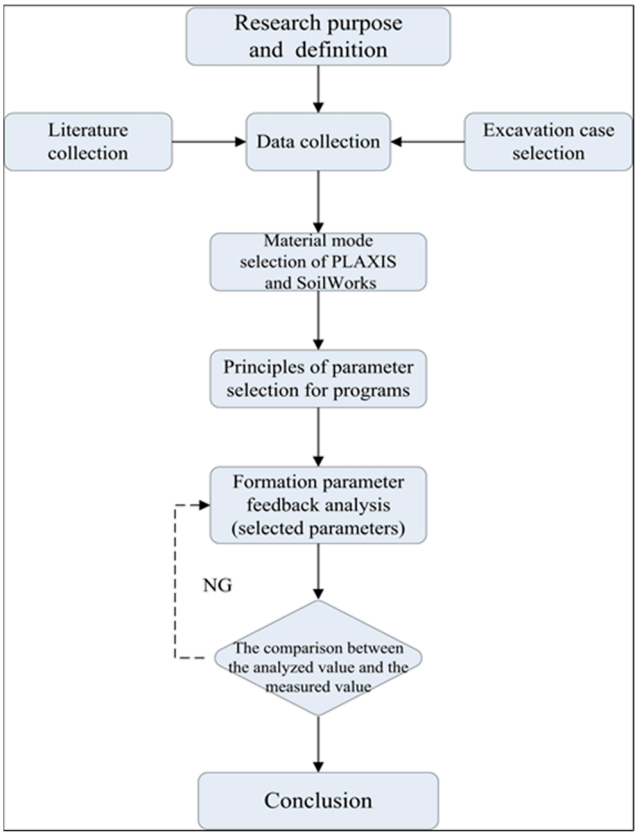


**Figure 1.** Flowchart of the research process.

### 2.2. Research Materials

- PLAXIS Numerical Simulation
  The background and characteristics of the PLAXIS program, along with an explanation of the numerical analysis model used, can be found in [4]. Case studies of gravel layer excavations in the Xindian area of New Taipei City were collected, and a feedback

analysis was performed using the existing monitoring data to derive suitable soil parameters for analysis using the PLAXIS program for the gravel layers.

- SoilWorks Numerical Simulation
  The background and characteristics of the SoilWorks program can be found in [34]. A sensitivity analysis was conducted using the basic case model and variations in the soil parameters adopted in previous studies, comparing the results with previous PLAXIS outcomes. The case study of gravel layer excavation in the Xindian area mentioned in the previous section was utilized to derive suitable soil parameters for analysis using the SoilWorks program. An additional case study, Case 3, was included for parameter verification.

## 3. PLAXIS Numerical Simulation

Most of the research literature on deep excavation focuses on soft soil and sandy soil, and there are relatively fewer results available regarding the engineering characteristics of gravel layers. Deep excavation engineering involves complex soil–structure interactions and can benefit from the application of relevant knowledge and experience from both the geotechnical and structural domains for design analysis. The aim of this study was to investigate the behavior of deep excavations in gravel layers in the Xindian area and provide reference parameters for deep excavation analysis and design in similar geological conditions by using collected monitoring data for feedback analysis.

The geological characteristics of gravel layers are mainly related to the size, shape, density, content, and properties of the gravel particles and the fine-grained material filling the voids. According to the findings of Hong et al., when the coarse material content (larger than sieve No. 4) in a gravel layer exceeds 75%, the engineering properties of the gravel layer are often determined by the characteristics of the coarse particles [35]. Conversely, if the content is less than 70%, the engineering properties are dominated by the fine-grained material. Das also pointed out that if coarse-grained soil contains more than 35% fine-grained material, it behaves more like a fine-grained material due to the sufficient filling of fine particles between the coarse particles, causing separation [36].

In this study, the case site was the upper part of the Jingmei gravel layer in the Xindian area. Due to its location in an urban area and limited investigation funds, it is difficult to find suitable sites for field testing. As a result, relevant test data are scarce. When conducting geotechnical engineering assessments, parameter values are usually estimated through empirical formulas based on field tests or assumed based on engineering experience. In this study, the parameters of the gravel layer were determined through actual monitoring data from case studies and referenced literature information. The feedback analysis helped to determine reasonable parameters for the gravel layer in practical cases, aiming to provide recommendations for the applicable range of the soil elastic modulus ($E_s$) parameters in the numerical analysis of deep excavation in the region.

### 3.1. Analysis Methods and Models

PLAXIS 2D software is used to address soil–structure interaction problems encountered in various geotechnical engineering applications. It can analyze behaviors such as deep excavation, slope stability, reinforced retaining walls, soil nails, ground anchors, internal bracing, raft foundations, pile foundations, seepage, tunnels, and other related issues, making it a powerful tool for geotechnical engineering analysis. PLAXIS provides multiple constitutive models for users to choose from to simulate the stress–strain behavior of soils.

Parameter Configuration and Modeling for Numerical Simulation Analysis

Due to space constraints in this paper, detailed content regarding the basic principles of PLAXIS is available in the user manual [4]. The following key points are summarized:

- Parameter Configuration

(1) Soil Parameters: In this study, the Mohr–Coulomb model, which is a built-in model within PLAXIS, was selected to simulate the soil behavior. The Mohr–Coulomb model is an elastic–perfectly plastic failure model based on elastoplastic theory. It considers factors such as the satisfaction of Hook's Law during the elastic stage, yielding criteria, and the flow rule. The soil parameters required for this model are explained as follows:

- Elastic modulus (*Es*): In general, the soil can be assigned an elastic modulus of 50% of the ultimate strength, known as the secant modulus (*E*50).
- Poisson's ratio ($\nu$): In most cases, the value of ν for soils ranges between 0.3 and 0.4.
- Cohesion ($c$): According to the PLAXIS user manual, a value of c greater than 0.2 kPa can be input for computational convenience.
- Internal friction angle ($\Phi$): The internal friction angle of the soil can be determined based on the soil type and shear strength tests conducted in the field or laboratory.
- Dilation angle ($\psi$): For cohesive soils, the dilation angle can be assumed to be 0. In the case of sandy soils, the angle is very small and sometimes even close to zero or negative ($\psi \fallingdotseq 0^\circ$ or $\psi < 0^\circ$); therefore, it can be assumed as $\psi = 0^\circ$ during the analysis.

By utilizing the Mohr–Coulomb model with the specified soil parameters, PLAXIS facilitates the simulation of soil behavior in this study.

(2) Retaining Structure Parameters

The retaining structure parameters are referenced from the original design calculations. It should be noted that different types of retaining walls have varying input parameters required for numerical analysis (refer to Section 3.2.4 for detailed research).

- Boundary Conditions for Numerical Analysis Modeling

In addition to the configuration of the relevant important parameters mentioned above, the determination of the boundary conditions is a crucial aspect of the simulation process. Factors that may affect the boundaries include $W_T$ (boundary width), $E_w$ (full cross-section excavation width), $e_w$ (half of the excavation width), $E_D$ (final excavation depth), and $D_T$ (boundary depth).

In the context of boundary considerations, domestic scholars Ou [37] and Chuung [38] have proposed different boundary conditions for reference. From an international perspective, scholars such as Maleki et al. have stated: "The distance from the lateral boundary of the model and the distance between the lower bound of the model from the top should be taken as sufficient so that the effects of the boundaries in the numerical model on the results are minimized. The displacement and the stress contours in the finite element software indicate that this distance is sufficient" [39–41].

### *3.2. Case Analysis*

#### 3.2.1. Case Study 1

- Site Description The site is located on the south side of Minquan Road, Xindian District, New Taipei City, with an area of approximately 8522 $m^2$. The site has an irregular shape, and the terrain varies within 1 m (Geotechnical Engineering Co., Ltd., New Taipei City, Taiwan. [42]).
- Subsurface Strata The subsurface strata at the site can be simplified into five layers from top to bottom, as described by Lin [43] and Geotechnical Engineering Co., Ltd. [44]. The simplified engineering parameters of the strata are shown in Table A1. The groundwater level at the site is approximately 10.7 to 11.3 m below the ground surface, and the groundwater pressure in the fifth layer of gravel is around 11.4 to 11.6 m below the ground surface, which is close to the free water level. For analysis purposes, the initial groundwater level is set at 11 m below the ground surface.
- Foundation Excavation Planning

(1) Geotechnical facilities: The foundation excavation has a depth of 17.30 m and utilizes a raft foundation. The retaining structure consists of a continuous wall with a thickness of 70 cm, and the wall depth is 27 m.
(2) Internal bracing system: The excavation follows a top-down sequence with staged excavation and horizontal bracing. The bracing system consists of five levels, using H-beams as support structures. The excavation profile is shown in Figure A1a.
(3) Excavation steps: The first stage involves excavation to GL.−2.7 m, followed by the installation of the first-level bracing. The second stage involves excavation to GL.−4.7 m and the installation of the second-level bracing. The third stage involves excavation to GL.−7.1 m and the installation of the third-level bracing. The fourth stage involves excavation to GL.−10.4 m and the installation of the fourth-level bracing. The fifth stage involves excavation to GL.−13.7 m and the installation of the fifth-level bracing. Finally, the sixth stage involves excavation to the final excavation bottom at GL.−17.3 m.

#### 3.2.2. Case Study 2

- Description of the Current Situation The site is located on the east side of Zhongzheng Road, Xindian District, New Taipei City, adjacent to Minquan Road, with an area of approximately 4560 $m^2$. It has an irregular shape, and the terrain varies within a range of 1 m (Geotechnical Engineering Co., Ltd. [45]).
- Subsurface Strata The subsurface strata at the site can be divided into five layers from top to bottom, as described by Lin [43] and Geotechnical Engineering Co., Ltd. [46]. The simplified engineering parameters of the strata are shown in Table A2. The groundwater investigation data at the site indicate that the groundwater level is typically around GL.−11 m. For analysis purposes, the initial groundwater level is set at 11 m below the ground surface.
- Foundation Excavation Planning
  (1) Geotechnical facilities: The foundation excavation has a depth of 13 m and utilizes a raft foundation. The retaining structure consists of a continuous wall with a thickness of 60 cm, and the wall depth is 20 m.
  (2) Internal bracing system: The excavation follows a top-down sequence with staged excavation and horizontal bracing. The bracing system consists of three levels, using H-beams as support structures. The excavation profile is shown in Figure A1b.
  (3) Excavation steps: The first stage involves excavation to GL.−2.6 m and the installation of the first-level bracing. The second stage involves excavation to GL.−6.0 m and the installation of the second-level bracing. The third stage involves excavation to GL.−9.3 m and the installation of the third-level bracing. The fourth stage involves excavation to the final excavation bottom at GL.−13.0 m. Due to the lower groundwater level in the research case area, the excavation depth mainly consists of the gravel layer, resulting in lower lateral pressures on the retaining wall compared to typical cases.

#### 3.2.3. Assumptions for Analysis

- The excavation process is assumed to exhibit plane strain behavior.
- Referring to the analysis model proposed by Fan, the influence range of the backside of the retaining wall is considered [47]. For the analysis, the range (B) extends at least four times the excavation depth beyond the retaining wall. The vertical range (D) is determined by adding twice the penetration depth (3H1 + H2) to the length of the continuous wall, assuming a uniform distributed load of 1.5 $t/m^2$ acting on the ground surface.
- Based on the site conditions, considering the excavation depth, plan shape, support system configuration, and soil layer boundaries, an analysis mesh is established.

The boundary elements of the mesh are assumed to have no horizontal or lateral displacements outside the influence range.

- The stiffness of the retaining wall is reduced by 70% based on general empirical values.
- The continuous wall and support elements are simulated using beam elements.
- An analysis is performed using 15-node triangular elements.
- At the bottom of the wall, if there is penetration into rock or gravel layers beyond a certain depth (more than 1.5 m), based on the reference monitoring data from relevant cases, no significant horizontal displacements are observed; therefore, in the analysis, horizontal displacements are constrained at the bottom of the wall.

#### 3.2.4. Determination of Strata and Structural Parameters

In this study, the elastic modulus ($E_s$) of the gravel layer was considered as a variable, ranging from 7840 N/m$^2$ to 9800 N/m$^2$. The remaining soil parameters and set values are presented in Tables 1 and A1 for Case Study 1, and Tables 2 and A2 for Case Study 2. The structural elements, such as the continuous wall and supports, were simulated using beam elements, and the main input data included a cross-sectional area (A), Young's modulus ($E$), moment of inertia ($I$), etc. The stiffness of the retaining wall was generally reduced by 70%. The basic parameters of the structural elements for Case Study 1 can be found in Tables 3 and 4, while for Case Study 2, they are presented in Tables 5 and 6.

**Table 3.** Diaphragm wall strength parameter input form of Case 1.

| Thickness (m) | $E$ (kN/m$^2$) | $I$ (m$^4$/m) | Reduction Factor | 0.7$EA$ (kN/m) | 0.7$EI$ (kNm$^2$/m) |
|---|---|---|---|---|---|
| 0.7 | $2.35 \times 10^7$ | 0.028583 | 0.7 | $1.13 \times 10^7$ | $4.60 \times 10^5$ |

**Table 4.** Support parameter input form of Case 1.

| Number of Supporting Layers | Supporting Position | Model | $A$ (cm$^2$) | 0.7$EA$ (kN) | Preload (kN/m) |
|---|---|---|---|---|---|
| 1ST | GL.−1.9 m | 1 × H 350 | 173.9 | $2.51 \times 10^6$ | 65 |
| 2ST | GL.−3.9 m | 1 × H 400 | 218.7 | $3.15 \times 10^6$ | 131 |
| 3ST | GL.−6.3 m | 1 × H 400 | 218.7 | $3.15 \times 10^6$ | 196 |
| 4ST | GL.−9.6 m | 2 × H 400 | 437.4 | $6.30 \times 10^6$ | 245 |
| 5ST | GL.−12.9 m | 2 × H 400 | 437.4 | $6.30 \times 10^6$ | 245 |

**Table 5.** Diaphragm wall strength parameter input table for Case 2.

| Thickness (m) | $E$ (kN/m$^2$) | $I$ (m$^4$/m) | Reduction Factor | 0.7$EA$ (kN/m) | 0.7$EI$ (kNm$^2$/m) |
|---|---|---|---|---|---|
| 0.6 | $2.35 \times 10^7$ | 0.018 | 0.7 | $9.66 \times 10^6$ | $2.90 \times 10^5$ |

**Table 6.** Support parameter input form of Case 2.

| Number of Supporting Layers | Supporting Position | Model | $A$ (cm$^2$) | 0.7$EA$ (kN) | Preload (kN/m) |
|---|---|---|---|---|---|
| 1ST | GL.−1.8 m | 1 × H 350 | 173.9 | $2.51 \times 10^6$ | 82 |
| 2ST | GL.−3.9 m | 1 × H 400 | 218.7 | $3.15 \times 10^6$ | 131 |
| 3ST | GL.−8.5 m | 1 × H 428 | 360.65 | $5.20 \times 10^6$ | 163 |

#### 3.2.5. Analysis Procedure

Due to the complexity of the actual excavation process on-site, numerical simulations often simplify the actual excavation steps by considering the influencing factors, such as monitoring data and construction conditions. Prior to the excavation simulation, it is commonly assumed that the continuous wall has been constructed, and the effects of

the wall construction on the strata are not considered. The groundwater level within the site is lowered to 1.0 m below the excavation surface during excavation operations. The construction processes for each case study are described as follows:

1. Case Study 1
   (1) First-stage excavation to GL.−2.7 m;
   (2) Installation of ST1 at GL.−1.9 m;
   (3) Second-stage excavation to GL.−4.7 m;
   (4) Installation of ST2 at GL.−3.9 m;
   (5) Third-stage excavation to GL.−7.1 m;
   (6) Installation of ST3 at GL.−6.3 m;
   (7) Fourth-stage excavation to GL.−10.4 m;
   (8) Installation of ST4 at GL.−9.6 m;
   (9) Fifth-stage excavation to GL.−13.7 m;
   (10) Installation of ST5 at GL.−12.9 m;
   (11) Sixth-stage excavation to the final excavation bottom at GL.−17.3 m (analysis mode ends at this point).
2. Case Study 2
   (1) First-stage excavation to GL.−2.6 m;
   (2) Installation of ST1 at GL.−1.8 m;
   (3) Second-stage excavation to GL.−6.0 m;
   (4) Installation of ST2 at GL.−5.2 m;
   (5) Third-stage excavation to GL.−9.3 m;
   (6) Installation of ST3 at GL.−8.5 m;
   (7) Fourth-stage excavation to the final excavation bottom at GL.−13.0 m (analysis and simulation end at this point).

#### 3.2.6. Feedback Analysis

Feedback analysis can generally be categorized into two approaches: the inverse approach and the direct approach. The inverse approach involves assuming a reasonable soil material composition model and using mathematical methods to express displacements as functions of in situ stresses and deformations. It then calculates the in situ stresses and modulus of deformation based on the displacement values. The direct approach involves continuously adjusting the input parameters for analysis and comparing the analysis results with the measured values until an acceptable range of error is achieved. While the inverse approach is faster in execution, it often requires simplification of materials into homogeneous and elastic conditions, resulting in poor performance for nonlinear materials. In contrast, the direct approach allows for a nonlinear analysis and considers material nonlinearity and elastoplastic behavior; therefore, the direct approach was adopted in this study and PLAXIS software was utilized as the analysis tool to simulate the stress–strain behavior of the foundation excavation.

The analysis focuses only on the final excavation stage for simulation and comparison. In both case studies, the second layer of the gravel layer has an $N$-value greater than 50; therefore, an $N$-value of 100 was assumed. The analysis was conducted by gradually increasing or decreasing the elastic modulus ($E_s$) of the soil. The analysis results for the final excavation stage using PLAXIS are shown in Figure 2a,b for Case Study 1 and in Figure 3a,b for Case Study 2.

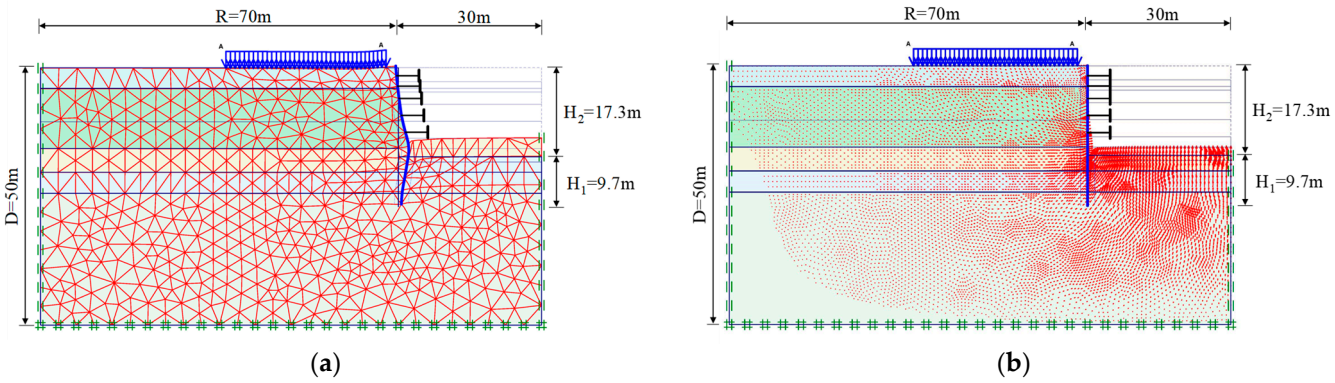


**Figure 2.** The final excavation stage of Case 1: (**a**) numerical mesh deformation during the final excavation stage and (**b**) overall displacement vector.

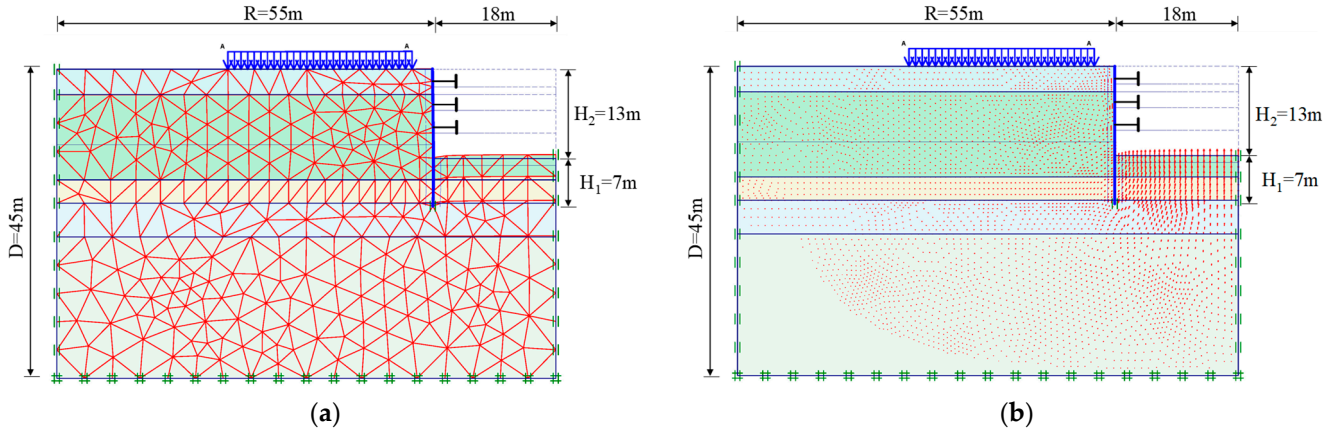


**Figure 3.** The final excavation stage of Case 2: (**a**) numerical mesh deformation during the final excavation stage and (**b**) overall displacement vector.

#### 3.2.7. Results and Discussion of the Case Studies

Based on the PLAXIS analysis results for the final excavation stage, the actual deformation curve data of the wall were compared to determine if the wall deformation was within a reasonable range of estimation. In this study, a maximum deformation tolerance of ±10% based on actual monitoring data was considered reasonable. The obtained results are shown in Figure 4a,b. The following discussion is based on the analysis results.

- Referring to the case studies in this research and numerous monitoring data, it was observed that when the bottom of the wall penetrates into a rock layer or gravel layer at a certain depth (greater than 1.5 m), there is no horizontal displacement at the bottom of the wall; therefore, in the analysis, the horizontal displacement at the bottom of the wall is restrained. The analysis results show consistency with the actual monitoring data in terms of the maximum deformation location and the trend of the wall displacement curve, indicating that this basic assumption of the analysis is reasonable.
- The feedback results from both case studies indicate that assuming an *N*-value of 100 for the second layer of the gravel layer, within the range of the soil elastic modulus between 7840 kN/m$^2$ and 9800 kN/m$^2$, it is possible to reasonably estimate the maximum deformation and its occurrence location during the final excavation stage, with a tolerance of ±10% based on the actual monitoring data.

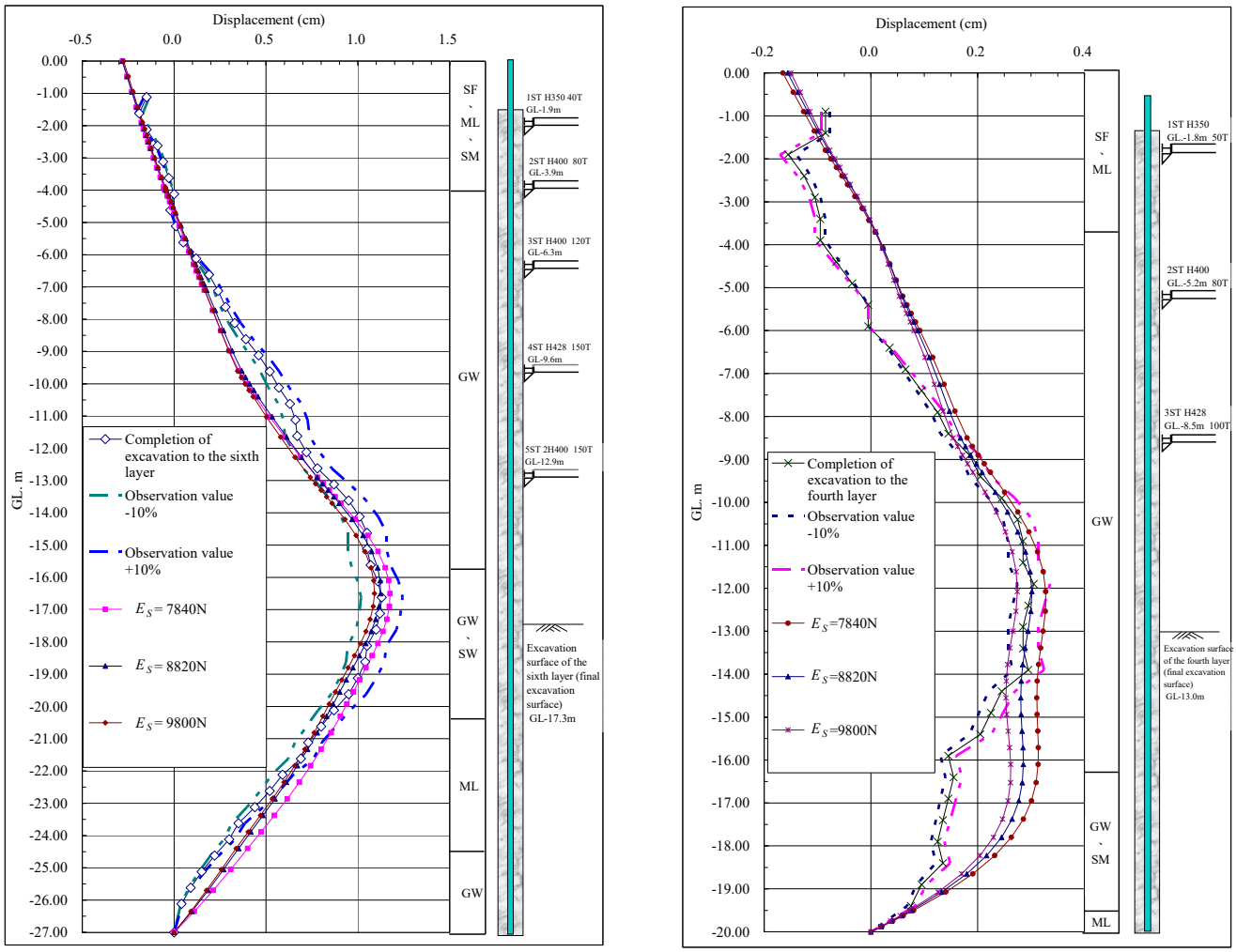


**Figure 4.** Comparison diagram of lateral displacement in the final excavation stage of (**a**) Case 1 and (**b**) Case 2.

### *3.3. Discussion of the Findings*

In this study, the PLAXIS 2D analysis program was used for a deep excavation parameter feedback analysis, and the results were compared with the actual monitoring data of the wall displacement. The analysis results show good agreement in terms of the trend of wall displacement and the location of maximum wall displacement, indicating the reasonability of this simulation approach. Based on the research findings, the following conclusions can be drawn:

- Based on the feedback analysis results from actual cases, it is shown that when using a reasonable soil elastic modulus for predictive analysis, more accurate final excavation deformation quantities can be obtained. In the Xindian area, this range is between 7840 kN/m$^2$; and 9800 kN/m$^2$;. These results align with the empirical formulas derived from the prior research of Kuo et al. and Hou et al. on the gravel layer in Baguashan. The elastic modulus in Baguashan was found to range from 88,200 kN/m$^2$; to 833,000 kN/m$^2$; [48,49].
- In this study, a parameter feedback analysis was conducted based on actual cases in the Xindian area of Taiwan, suggesting that this research method can be applied to regions with similar geological conditions. Extending this approach to various regions can yield a broader range of research results, which could be valuable as references in engineering design.

## 4. SoilWorks Numerical Simulation

The SoilWorks program is a two-dimensional geotechnical engineering analysis and design package developed by MIDAS Corporation in collaboration with scholars and industry professionals in the field of soil and rock [34]. It incorporates MIDAS IT's unique graphical processing, meshing, and numerical analysis techniques, along with the latest analysis and design technologies in areas such as tunnels, slopes, weak ground treatment, foundations, seepage, and dynamic analysis. It has become an essential tool for the academic and professional engineering community. The program consists of seven major analysis modules, including finite element stress–strain, excavation deformation, slope stability, seepage, consolidation, pile, and dynamic modules.

### *4.1. Analysis Methods and Models*

The selection of material constitutive models has a significant impact on the analysis results, such as material behavior, stress, and strain. SoilWorks provides various geotechnical constitutive models for users to choose from in order to simulate the stress–strain behavior of soils.

The Mohr–Coulomb model is commonly used to simulate geotechnical materials. Figure 5a shows the idealized elastic–plastic characteristics. Under this assumption, reliable results can be obtained in general geotechnical nonlinear analyses; therefore, in this study, the Mohr–Coulomb model was also used for relevant numerical analysis work.

The Mohr–Coulomb yield criterion has two limitations in simulating soil material behavior. The first limitation is the assumption that the second principal stress has no effect on the yield, which does not match the experimental results. The second limitation is that the meridians of the Mohr circle and the yield envelope are straight lines, and the strength parameters do not vary with the confining pressure or pore water pressure (see Figure 5b); therefore, this constitutive model is more accurate when there is minimal variation in the confining pressure but loses accuracy when there is significant variation. Additionally, the yield surface has corners, leading to errors in numerical analysis; however, this criterion provides good accuracy under commonly encountered confining pressures and has become the most commonly adopted failure criterion, effectively solving most numerical analysis problems in geotechnical engineering.

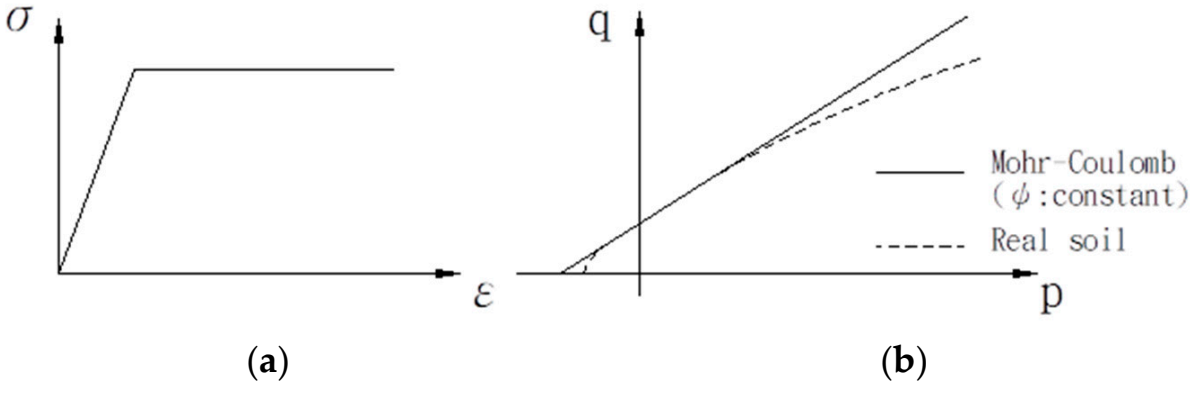


**Figure 5.** (**a**) Material properties; (**b**) yield function of the Mohr–Coulomb model.

The soil material parameters required for the Mohr–Coulomb model include the elastic modulus, Poisson's ratio, cohesion, the friction angle, the dilation angle, the bulk modulus, and the elastic shear modulus, totaling seven parameters.

### *4.2. Sensitivity Analysis*

#### 4.2.1. Analysis Description

From the relevant academic and engineering research literature or analysis reports, it is known that certain key parameters must be appropriately adjusted to obtain reasonable

results. The values of the geotechnical parameters and data, such as the groundwater level and pore pressure used in the analysis, can mostly be obtained through field drilling and general physical and mechanical experiments, with relatively small variations. Among the required input values, the effective friction angle and soil elastic modulus are the most crucial parameters in the finite element program. The effective friction angle needs to consider the influence of field sampling operations and excavation disturbance, while the soil elastic modulus has numerous empirical formulas developed over the years, resulting in a larger range of variation.

In this study, sensitivity analyses were conducted on the effective friction angle of the soil strength parameters and the soil elastic modulus of the ground reaction parameters. The aim was to discuss the results quantitatively and compare them with the analysis results from the PLAXIS program in the previous section.

#### 4.2.2. Assumed Cases

To understand the sensitivity of the geological parameters on the displacement, stress, or axial force of the retaining wall in the SoilWorks program, reference is made to the cases studied by Hsieh et al. [24] and Qiu et al. [26] using the RIDO and PLAXIS programs, respectively. Hypothetical cases representing sand and clay soils are established for the subsequent sensitivity analysis.

- Basic Case Description for Sandy Soil Layer
  - (1) Analysis Assumptions
    - A. The length and width of the excavation area are both 40 m, with a depth of excavation of 12 m (H1) and a depth of wall penetration of 10 m (H2). The total length of the continuous wall is 22 m.
    - B. The analysis model adopts a symmetric single-side mode, with a horizontal analysis length (B) of half the original excavation length, which is 20 m. Considering the influence range of the backside of the retaining wall, a distance of at least four times the excavation depth (R = 12 × 4 = 48 m) is considered. The vertical range (D) is taken as the length of the continuous wall (H1 + H2) plus twice the penetration depth (H2), assuming a uniformly distributed load of 10 kN/m$^2$ acting on the ground surface. The detailed model diagram for the simulated case analysis is shown in Figure 6.
    - C. Considering the excavation depth, support system configuration, and soil layer boundaries, a complete analysis mesh is established. The boundary elements of the mesh are assumed to have no horizontal or lateral displacements outside the influence range.
    - D. The retaining wall is simulated using beam elements, with the stiffness reduced by 70% based on general empirical values. The input parameters used in the analysis are detailed in Table A3.
    - E. The support system is simulated using truss elements, with the stiffness reduced by 50% based on general empirical values. The input parameters used in the analysis are detailed in Table A4.
    - F. The analysis is conducted using 15-node triangular elements.
  - (2) Geology and Groundwater

The sandy soil layer is divided into layers with a thickness of 10 m each. There are a total of 5 layers, and the soil parameters for each layer are detailed in Table A5. The initial groundwater level is assumed to be 1 m below the ground surface.

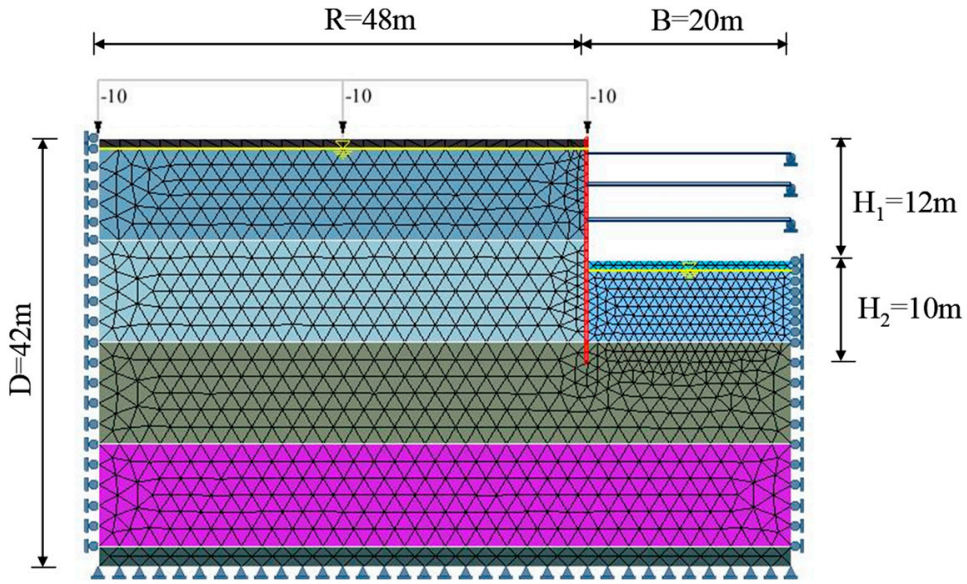


**Figure 6.** Case analysis model for sandy soil layer simulation.

- Basic Case Description for Clay Soil Layer

(1) Analysis Assumptions

A. The length and width of the excavation area are both 40 m, with a depth of excavation of 12 m (H1) and a depth of wall penetration of 12 m (H2). The total length of the continuous wall is 24 m.

B. The analysis model adopts a symmetric single-side mode, with a horizontal analysis length (B) of half the original excavation length, which is 20 m. Considering the influence range of the backside of the retaining wall, a distance of at least four times the excavation depth (R = 12 × 4 = 48 m) is considered. The vertical range (D) is taken as the length of the continuous wall (H1 + H2) plus twice the penetration depth (H2), assuming a uniformly distributed load of 10 kN/m$^2$ acting on the ground surface. The detailed model diagram for the simulated case analysis is shown in Figure 7.

C. Considering the excavation depth, support system configuration, and soil layer boundaries, a complete analysis mesh is established. The boundary elements of the mesh are assumed to have no horizontal or lateral displacements outside the influence range.

D. The retaining wall is simulated using beam elements, and the input parameters used in the analysis are detailed in Table A3.

E. The support system is simulated using truss elements, and the input parameters used in the analysis are detailed in Table A4.

F. An analysis is conducted using 15-node triangular elements.

(2) Geology and Groundwater

The clay soil layer is divided into layers with a thickness of 10 m each. There are a total of 5 layers, and the soil parameters for each layer are detailed in Table A6. The initial groundwater level is assumed to be 1 m below the ground surface. For the analysis of the clay soil layer, the drainage and undrained conditions are considered based on the cases presented by Qiu et al. [26].

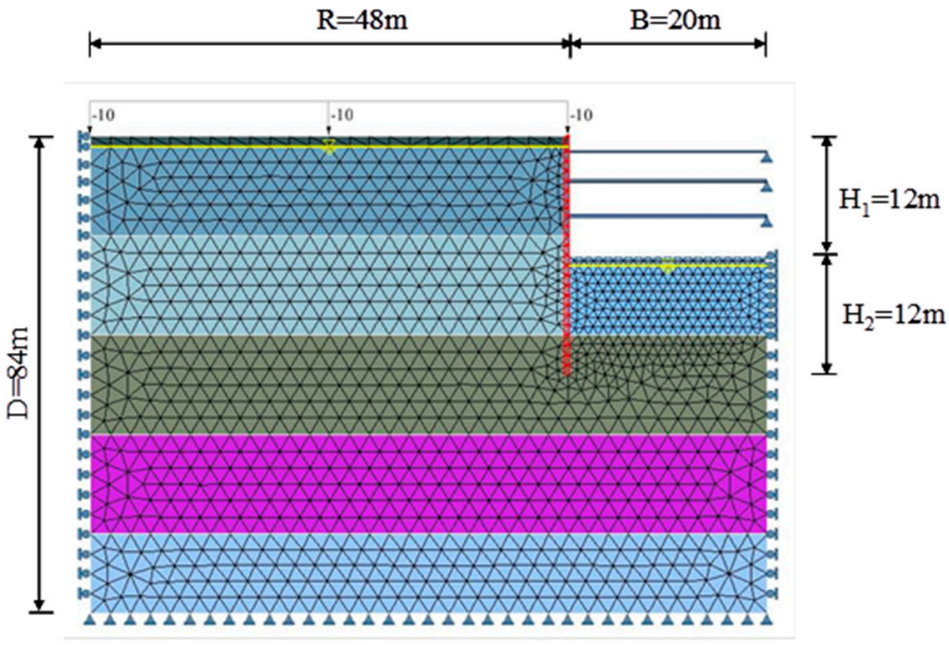


**Figure 7.** Case analysis model for clay layer simulation.

4.2.3. Parameter Range

Based on previous studies, the ranges of the effective friction angle and soil elastic modulus are as follows:

- Friction Angle ($\Phi$)

For the analysis of sandy soils, the effective stress analysis ($C$ = 0) is commonly used. In this study, the simulated analysis considers the variation of the friction angle by 80%, 90%, 100%, 110%, and 120% of the original assumed friction angle. These values are based on the research methods of Zhang et al. [25] and Qiu et al. [26].

- Soil Elastic Modulus ($E_s$)

From the literature in the previous section, it is known that there are numerous empirical formulas for the soil elastic modulus, and the difference between the maximum and minimum values can be several times. In this simulation, the analysis considers the variation of the soil elastic modulus by 50%, 75%, 100%, 150%, and 200% of the original assumed soil elastic modulus. These values are based on the research methods of Zhang et al. [25] and Qiu et al. [26].

4.2.4. Analysis Results

- Sensitivity Analysis of Friction Angle

The results for different assumed geological conditions, including sandy soil and clay (drained and undrained) soil, were integrated and an integrated analysis was conducted. The maximum bending moment (*Mmax*), maximum displacement (*Dmax*), and average axial force (*Favg*) corresponding to the assumed friction angles of 80%, 90%, 100%, 110%, and 120% were compared with the maximum bending moment, maximum displacement, and average axial force at the original friction angle (100%). The percentage changes in the maximum bending moment, maximum displacement, and average axial force due to the variation in friction angle were calculated. The sensitivity of the friction angle ($\Phi$) on these three parameters (*Mmax*, *Dmax*, *Favg*) is discussed. The analysis results from Qiu et al.'s [26] PLAXIS program are also considered.

(1) Sandy Soil Layer

From the summarized analysis results in Table 7, it can be observed that when the friction angle varies from 80% to 120% of the baseline value (100%), the range of variation

in the maximum wall moment (*Mmax*) is 282.78 to 392.24 kN-m, with a percentage change of 88% to 121%. The range of variation in the maximum displacement (*Dmax*) is 29.664 to 40.840 mm, with a percentage change of 90% to 124%. The range of variation in the average axial force (*Favg*) is 223.3 to 278.8 kN/m, with a percentage change of 91% to 114%.

Line graphs depicting the percentage change in the three parameters (*Mmax*, *Dmax*, *Favg*) with respect to different friction angles ($\Phi$) were plotted. From Figure 8a, it can be observed that the friction angle has a significant sensitivity to *Dmax*, with an increase of 24% when $\Phi$ is decreased by 20%. When $\Phi$ is increased by 20%, *Mmax*, *Dmax*, and *Favg* decrease by approximately 10%. The results indicate that a smaller friction angle has a more significant effect on *Dmax*, while higher friction angles have similar influences on *Mmax*, *Dmax*, and *Favg*.

Additionally, the sensitivity analysis results for the friction angle in sandy soils from Qiu et al.'s [26] PLAXIS program were compared with the SoilWorks program. From Table 8 and Figures 8b and 9a,b, it can be observed that when the friction angle is smaller, the variation in the PLAXIS results is more significant compared to the SoilWorks program. This indicates that PLAXIS is more sensitive to the friction angle than the SoilWorks program.

(2) Clay Layer (Undrained Condition)

From the summarized analysis results in Table 9, it can be observed that when the friction angle varies from 80% to 120% of the baseline value (100%) in the undrained condition, the range of variation in the maximum wall moment (*Mmax*) is 243.96 to 267.27 kN-m, with a percentage change of 97% to 106%. The range of variation in the maximum displacement (*Dmax*) is 46.110 to 48.232 mm, with a percentage change of 98% to 103%. The range of variation in the average axial force (*Favg*) is 232.5 to 252.5 kN/m, with a percentage change of 96% to 105%.

Line graphs depicting the percentage change in the three parameters (*Mmax*, *Dmax*, *Favg*) with respect to different friction angles ($\Phi$) were plotted. From Figure 10a, it can be observed that the sensitivity of the friction angle ($\Phi$) on the clay layer (undrained condition) is relatively small, with changes of approximately 6% in *Mmax*, *Dmax*, and *Favg* when $\Phi$ is decreased or increased. The results indicate that the clay layer (undrained condition) is not particularly sensitive to the variation in friction angle.

Additionally, the sensitivity analysis results for the friction angle in the clay layer (undrained condition) from Qiu et al.'s [26] PLAXIS program were compared with the SoilWorks program. From Table 10 and Figures 10b and 11a,b, it can be observed that when the friction angle is increased, both programs show only a slight variation. When the friction angle is smaller, especially in terms of *Mmax* or *Dmax*, the variation in the PLAXIS program is more significant compared to the SoilWorks program, indicating that PLAXIS is more sensitive to the friction angle in the clay layer (undrained condition) when the friction angle is smaller.

**Table 7.** Sensitivity analysis results of friction angle for sandy layers.

| SM | *Mmax* | Percentage Change | *Dmax* | Percentage Change | *Favg* | Percentage Change |
|---|---|---|---|---|---|---|
| | (kN-m) | (%) | (mm) | (%) | (kN/m) | (%) |
| *0.8Φ* | 392.24 | 121% | 40.840 | 124% | 278.8 | 114% |
| *0.9Φ* | 353.90 | 110% | 36.116 | 110% | 260.4 | 106% |
| *1.0Φ* | 323.07 | 100% | 32.872 | 100% | 245.4 | 100% |
| *1.1Φ* | 300.21 | 93% | 30.852 | 94% | 233.4 | 95% |
| *1.2Φ* | 282.78 | 88% | 29.664 | 90% | 223.3 | 91% |

**Table 8.** Sensitivity of friction angle for sandy layers in PLAXIS and SoilWorks.

| SM | *Mmax* Percentage Change | | *Dmax* Percentage Change | | *Favg* Percentage Change | |
|---|---|---|---|---|---|---|
| | SoilWorks | PLAXIS | SoilWorks | PLAXIS | SoilWorks | PLAXIS |
| *0.8Φ* | 121% | 139% | 124% | 157% | 114% | 122% |
| *0.9Φ* | 110% | 117% | 110% | 119% | 106% | 108% |
| *1.0Φ* | 100% | 100% | 100% | 100% | 100% | 100% |
| *1.1Φ* | 93% | 89% | 94% | 91% | 95% | 96% |
| *1.2Φ* | 88% | 81% | 90% | 86% | 91% | 93% |

**Table 9.** Sensitivity analysis results of friction angle for clay layers (undrained).

| CL (Undrained) | *Mmax* | Percentage Change | *Dmax* | Percentage Change | *Favg* | Percentage Change |
|---|---|---|---|---|---|---|
| | (kN-m) | (%) | (mm) | (%) | (kN/m) | (%) |
| *0.8Φ* | 267.27 | 106% | 48.232 | 103% | 252.5 | 105% |
| *0.9Φ* | 256.45 | 102% | 47.333 | 101% | 246.1 | 102% |
| *1.0Φ* | 251.72 | 100% | 46.867 | 100% | 241.4 | 100% |
| *1.1Φ* | 246.78 | 98% | 46.424 | 99% | 236.8 | 98% |
| *1.2Φ* | 243.96 | 97% | 46.110 | 98% | 232.5 | 96% |

**Table 10.** Sensitivity of friction angle for clay layers (undrained) in PLAXIS and SoilWorks.

| CL (Undrained) | *Mmax* Percentage Change | | *Dmax* Percentage Change | | *Favg* Percentage Change | |
|---|---|---|---|---|---|---|
| | SoilWorks | PLAXIS | SoilWorks | PLAXIS | SoilWorks | PLAXIS |
| *0.8Φ* | 106% | 133% | 103% | 129% | 105% | 118% |
| *0.9Φ* | 102% | 112% | 101% | 110% | 102% | 107% |
| *1.0Φ* | 100% | 100% | 100% | 100% | 100% | 100% |
| *1.1Φ* | 98% | 93% | 99% | 95% | 98% | 97% |
| *1.2Φ* | 97% | 90% | 98% | 93% | 96% | 96% |

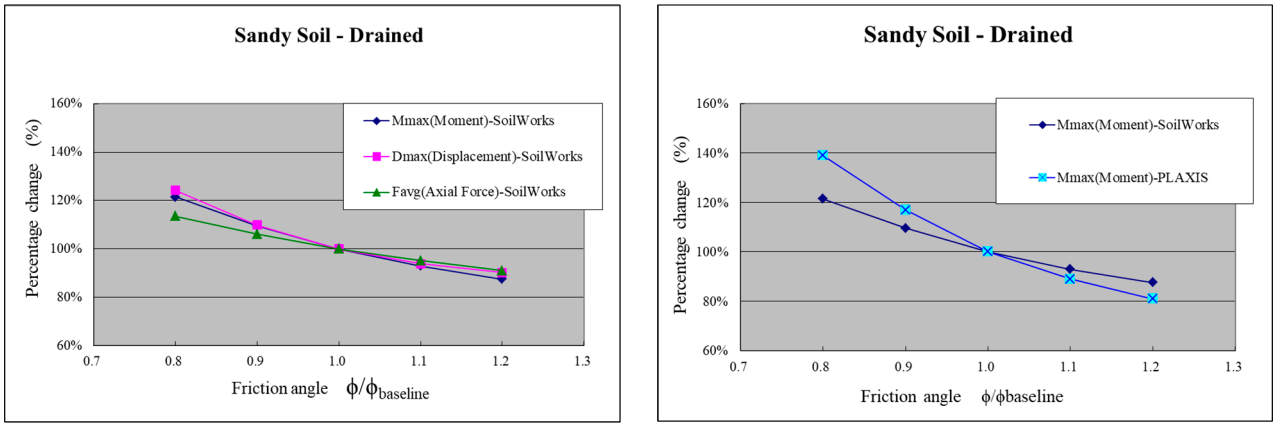


(**a**) (**b**)

**Figure 8.** Comparison of the sensitivity diagrams for sandy soil (drained): (**a**) SoilWorks programs compared for friction angle (*Mmax*, *Dmax* and *Favg*); (**b**) PLAXIS and SoilWorks programs compared for friction angle (*Mmax*).

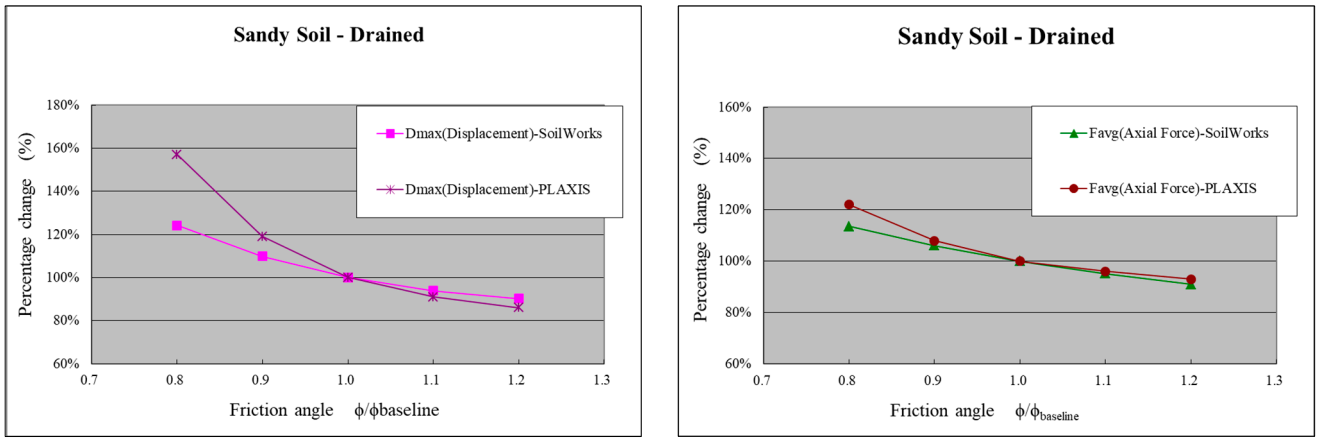


(**a**) (**b**)

**Figure 9.** Comparison of the sensitivity of PLAXIS and SoilWorks programs to sandy soil (drained): (**a**) friction angle (*Dmax*); (**b**) friction angle (*Favg*).

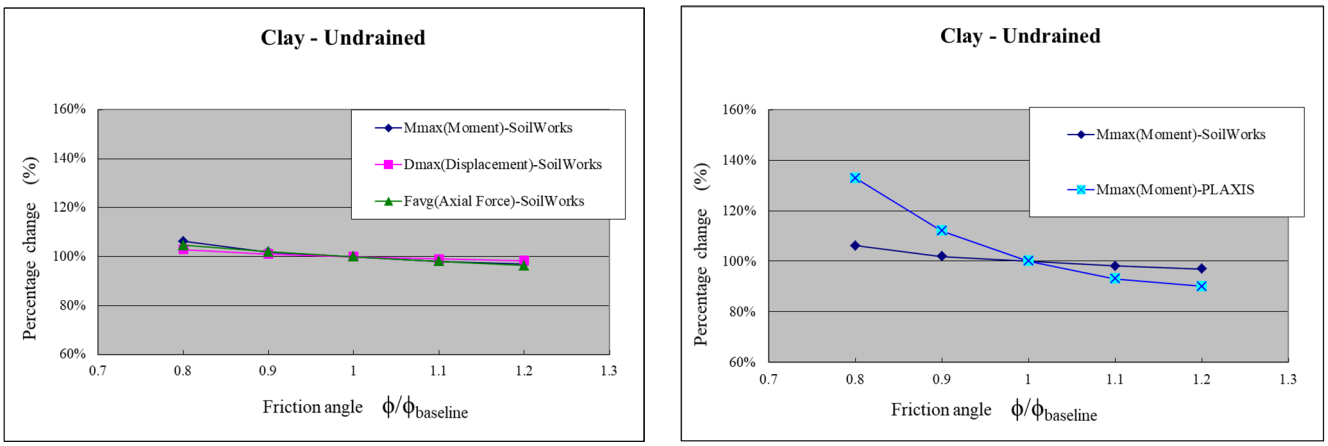


(**a**) (**b**)

**Figure 10.** Comparison of the sensitivity diagrams for clay (undrained): (**a**) SoilWorks programs compared for friction angle (*Mmax*, *Dmax* and *Favg*); (**b**) PLAXIS and SoilWorks programs compared for friction angle (*Mmax*).

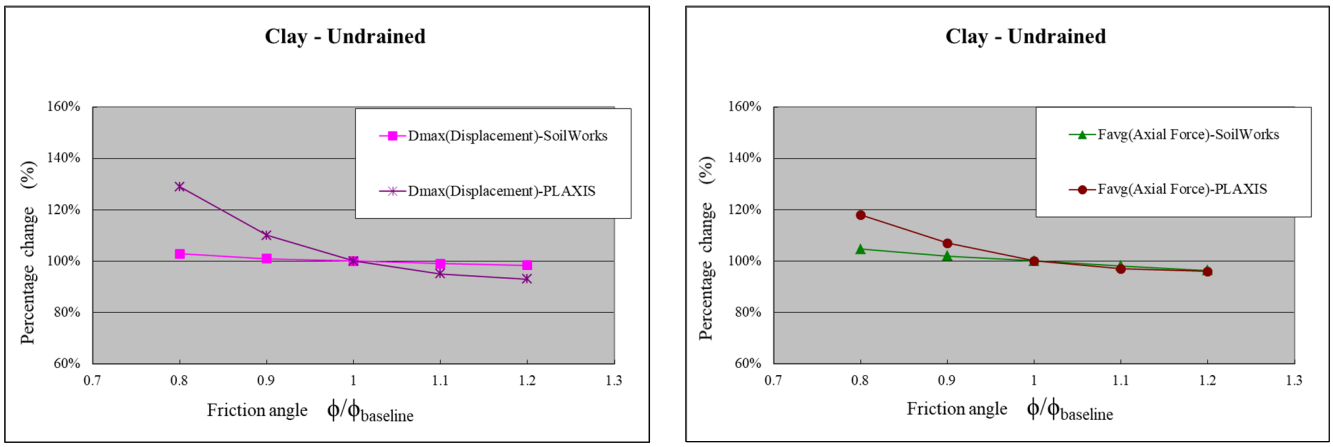


(**a**) (**b**)

**Figure 11.** Comparison of the sensitivity of PLAXIS and SoilWorks programs to clay (undrained): (**a**) friction angle (*Dmax*); (**b**) friction angle (*Favg*).

- Sensitivity Analysis of Soil Elastic Modulus

The results for different assumed geological conditions were integrated, including sandy soil and clay (drained and undrained) soil, and an integrated analysis was conducted. The maximum bending moment (*Mmax*), maximum displacement (*Dmax*), and average axial force (*Favg*) corresponding to the assumed soil elastic moduli of 50%, 75%, 100%, 150%, and 200% were compared with the maximum bending moment, maximum displacement, and average axial force at the original soil elastic modulus (100%). The percentage change in the maximum bending moment, maximum displacement, and average axial force due to the variation in soil elastic modulus was calculated. The sensitivity of the soil elastic modulus (*E*) on these three parameters (*Mmax*, *Dmax*, *Favg*) is discussed. The analysis results from Qiu et al.'s [26] PLAXIS program are also considered.

(1) Sandy Soil

From the summarized analysis results in Table A7, it can be observed that when the soil elastic modulus varies from 50% to 200% of the baseline value (100%) in sandy soil, the range of variation in the maximum bending moment (*Mmax*) is 280.69 to 371.32 kN-m, with a percentage change of 87% to 115%. The range of variation in the maximum displacement (*Dmax*) is 23.941 to 48.483 mm, with a percentage change of 73% to 147%. The range of variation in the average axial force (*Favg*) is 246.1 to 251.7 kN/m, with a percentage change of 100% to 103%.

Line graphs depicting the percentage change in the three parameters (*Mmax*, *Dmax*, *Favg*) with respect to different soil elastic moduli were plotted. From Figure 12a, it can be observed that the sensitivity of the soil elastic modulus (*Es*) in sandy soil is more significant for *Mmax* and *Dmax*, with *Dmax* showing a maximum increase of 47% when *E* is decreased by 50% and a maximum decrease of approximately 27% when *E* is increased by 200%. The results indicate that the variation in *Mmax* and *Dmax* is more pronounced when the soil elastic modulus is higher or lower, while the effect on Favg is relatively small.

Additionally, the sensitivity analysis results for the soil elastic modulus in sandy soil from Qiu et al.'s [26] PLAXIS program were compared with the SoilWorks program. From Table A8 and Figures 12b and 13a,b, it can be observed that PLAXIS is more sensitive to variations in *Dmax* than the SoilWorks program when the soil elastic modulus in sandy soil is smaller.

(2) Clay Layer (Undrained Condition)

From the summarized analysis results in Table A9, it can be observed that when the soil elastic modulus varies from 50% to 200% of the baseline value (100%) in the undrained condition of the clay layer, the range of variation in the maximum bending moment (*Mmax*) is 205.65 to 327.72 kN-m, with a percentage change of 82% to 130%. The range of variation in the maximum displacement (*Dmax*) is 28.341 to 81.231 mm, with a percentage change of 60% to 173%. The range of variation in the average axial force (*Favg*) is 231.2 to 257.0 kN/m, with a percentage change of 96% to 106%.

Line graphs depicting the percentage change in the three parameters (*Mmax*, *Dmax*, *Favg*) with respect to different soil elastic moduli were plotted. From Figure 14a, it can be observed that the sensitivity of the soil elastic modulus (*Es*) in the undrained condition of the clay layer is more significant for *Dmax*, with *Dmax* showing a maximum increase of 73% when *Es* is decreased by 50% and a maximum decrease of approximately 40% when *Es* is increased by 200%. The results indicate that the variation in *Dmax* is more pronounced when the soil elastic modulus is higher or lower, while the effect on *Favg* is relatively small.

Additionally, the sensitivity analysis results for the soil elastic modulus in the undrained condition of the clay layer from Qiu et al.'s [26] PLAXIS program were compared with the SoilWorks program. From Table A10 and Figures 14b and 15a,b, it can be observed that both programs show similar sensitivity to variations in *Mmax*, *Dmax*, and *Favg* when the soil elastic modulus in the undrained condition of the clay layer is considered, with *Dmax* exhibiting the most significant sensitivity.

(3) Clay Layer (Drained Condition)

From the summarized analysis results in Table A11, it can be observed that when the soil elastic modulus varies from 50% to 200% of the baseline value (100%) in the drained condition of the clay layer, the range of variation in the maximum bending moment (*Mmax*) is 327.66 to 439.21 kN-m, with a percentage change of 87% to 116%. The range of variation in the maximum displacement (*Dmax*) is 32.639 to 71.259 mm, with a percentage change of 70% to 152%. The range of variation in the average axial force (*Favg*) is 253.6 to 260.5 kN/m, with a percentage change of 99% to 102%.

Line graphs depicting the percentage change in the three parameters (*Mmax*, *Dmax*, *Favg*) with respect to different soil elastic moduli were plotted. From Figure 16a, it can be observed that the sensitivity of the soil elastic modulus (*Es*) in the drained condition of the clay layer is more significant for *Dmax*, with *Dmax* showing a maximum increase of 52% when *Es* is decreased by 50% and a maximum decrease of approximately 30% when *Es* is increased by 200%. The results indicate that the variation in *Dmax* is more pronounced when the soil elastic modulus is higher or lower, while the effect on *Favg* is relatively small.

Additionally, the sensitivity analysis results for the soil elastic modulus in the drained condition of the clay layer from Qiu et al.'s [26] PLAXIS program were compared with the SoilWorks program. From Table A12 and Figure 16b to Figure 17a,b, it can be observed that both programs show similar sensitivity to variations in *Mmax*, *Dmax*, and *Favg* when the soil elastic modulus in the drained condition of the clay layer is considered, with *Dmax* exhibiting the most significant sensitivity.

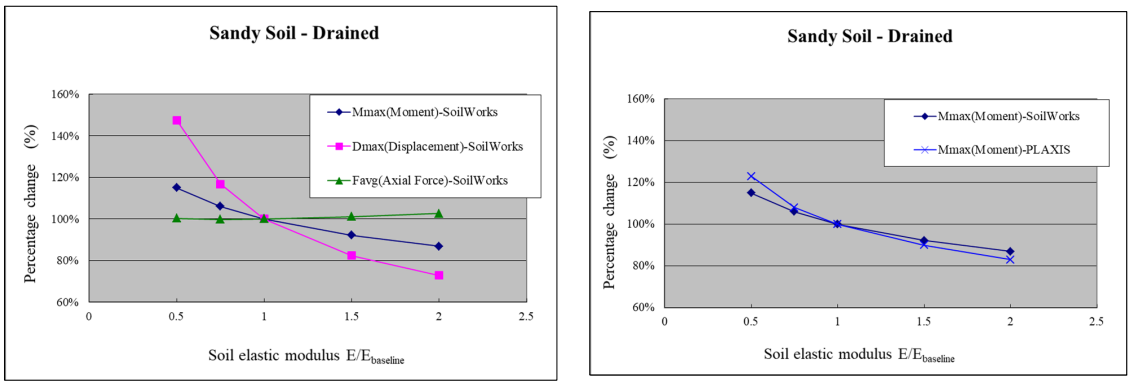


(**a**) (**b**)

**Figure 12.** Comparison of the sensitivity diagrams for sandy soil (drained): (**a**) SoilWorks programs compared for elastic modulus (*Mmax*, *Dmax* and *Favg*); (**b**) PLAXIS and SoilWorks programs compared for elastic modulus (*Mmax*).

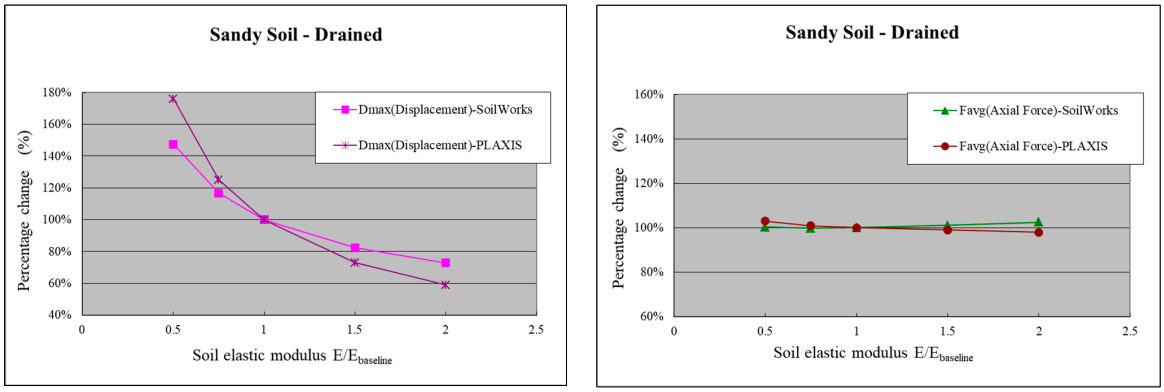


(**a**) (**b**)

**Figure 13.** Comparison of the sensitivity of PLAXIS and SoilWorks programs to sandy soil (drained): (**a**) elastic modulus (*Dmax*); (**b**) elastic modulus (*Favg*).

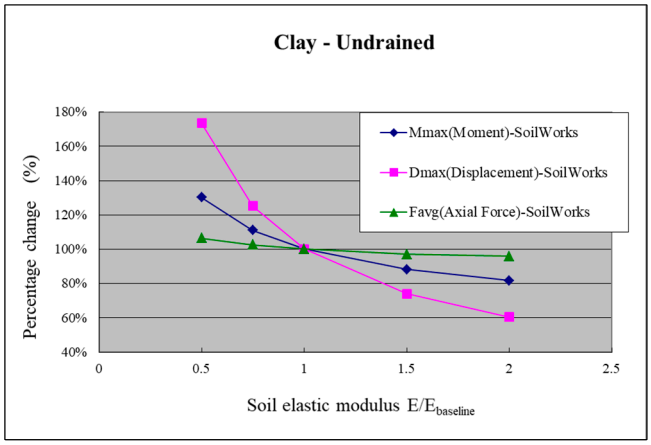


(**a**)

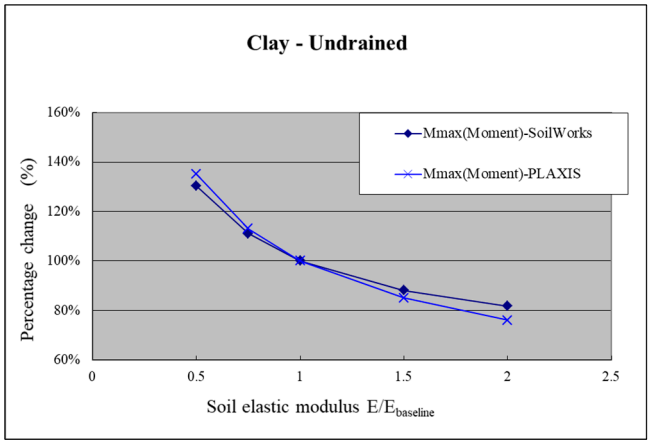


(**b**)

**Figure 14.** Comparison of the sensitivity diagrams for clay (undrained): (**a**) SoilWorks programs compared for elastic modulus (*Mmax*, *Dmax*, and *Favg*); (**b**) PLAXIS and SoilWorks programs compared for elastic modulus (*Mmax*).

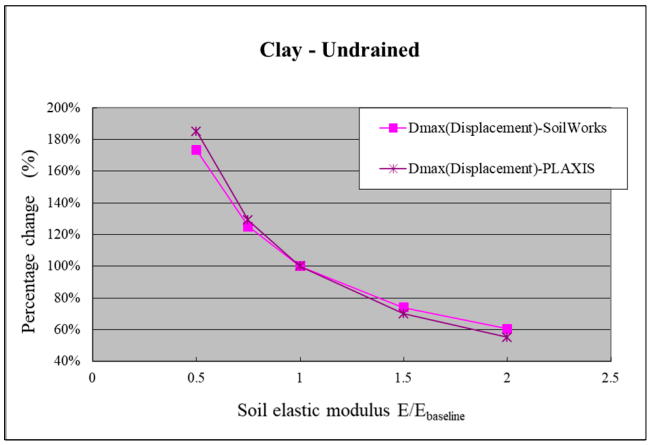


(**a**)

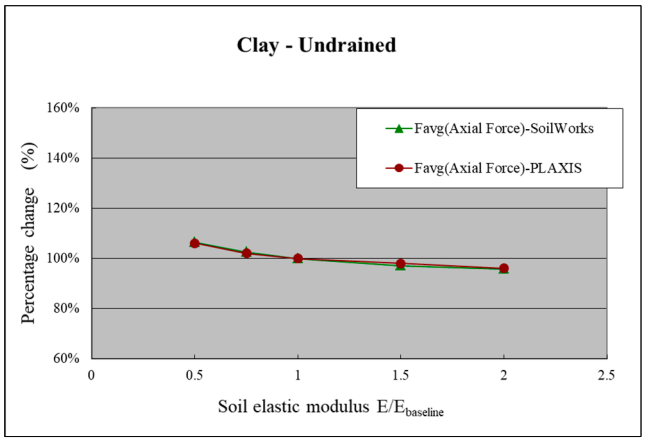


(**b**)

**Figure 15.** Comparison of the sensitivity of PLAXIS and SoilWorks programs to clay (undrained): (**a**) elastic modulus (*Dmax*); (**b**) elastic modulus (*Favg*).

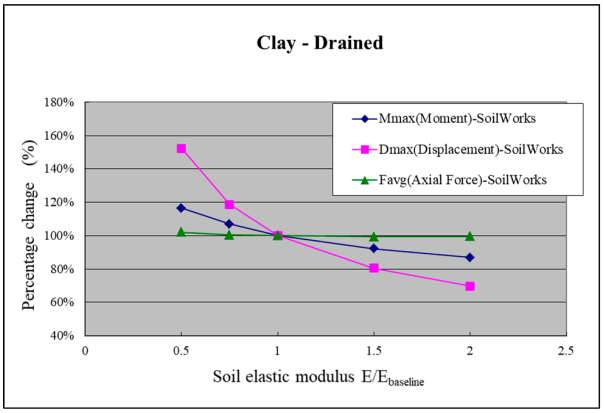


(**a**)

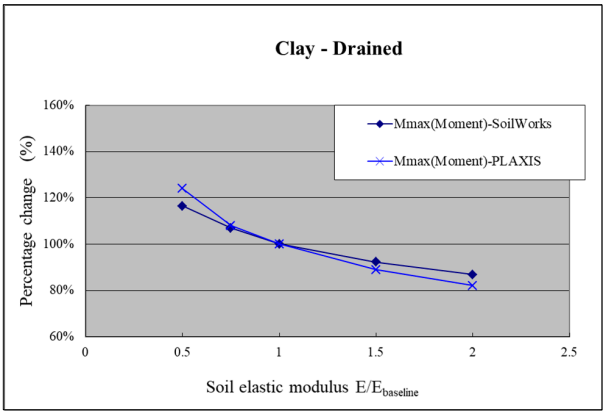


(**b**)

**Figure 16.** Comparison of the sensitivity diagrams for clay (drained): (**a**) SoilWorks programs compared for elastic modulus (*Mmax*, *Dmax*, and *Favg*); (**b**) PLAXIS and SoilWorks programs compared for elastic modulus (*Mmax*).

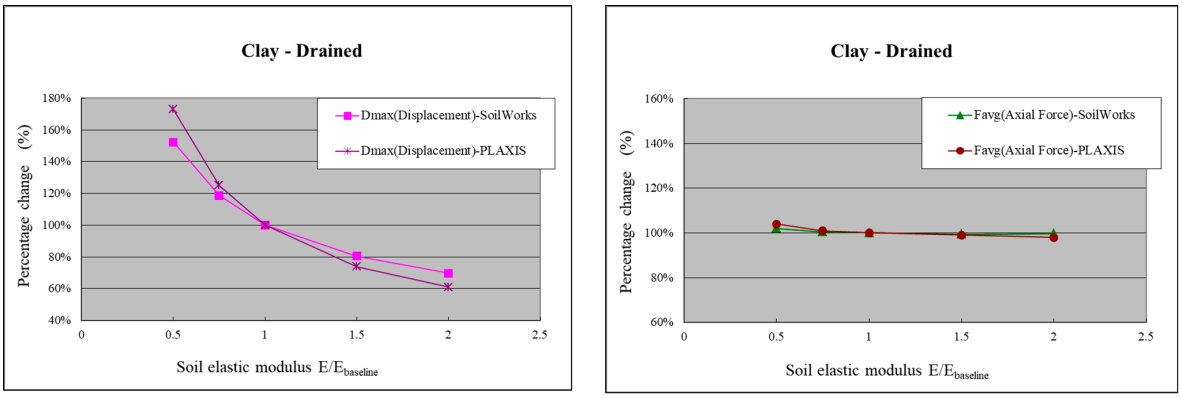


(**a**) (**b**)

**Figure 17.** Comparison of the sensitivity of PLAXIS and SoilWorks programs to clay (drained): (**a**) elastic modulus (*Dmax*); (**b**) elastic modulus (*Favg*).

### *4.3. Case Study*

In this study, a feedback analysis was conducted using one case, which followed the excavation and support method of six excavations with five-layer supports. The case was based on PLAXIS analysis Case 1 presented in Section 4. The geological input parameters used in the SoilWorks program for this case are shown in Table 11. The input parameters for the retaining wall and support system can be found in Tables 3 and 4, respectively. The analysis process is described in Section 4.3.1. The analysis model is illustrated in Figure 18.

To verify the suitability of the range of elastic modulus values used for the gravel layer in the program based on the feedback from Case 1, an additional case (Case 3) is introduced for validation.

**Table 11.** Soil strength parameter input table for Case Study 1 in SoilWorks.

| Depth (m) | Soil Classification | Use *N* Value | $c'$ (kN/m$^2$) | $\Phi'$ (°) | $\gamma_{unsat}$ (kN/m$^3$) | $\gamma_{sat}$ (kN/m$^3$) | $E_S$ (kN/m$^2$) | $\nu$ |
|---|---|---|---|---|---|---|---|---|
| 0.0~4.0 | SF, ML, SM | 5 | 0 | 30 | 19.3 | 19.5 | 12,250 N | 0.33 |
| 4.0~15.7 | GW | 40 | 4.9 | 38 | 21.8 | 22.0 | 2450 N–3430 N | 0.28 |
| 15.7~20.3 | GW, SW | 35 | 0 | 38 | 21.1 | 21.4 | 2450 N–3430 N | 0.28 |
| 20.3~24.4 | ML | 16 | 0 | 32 | 19.4 | 19.7 | 39,200 N | 0.32 |
| 24.4~33.0 | GW | 100 | 9.8 | 40 | 22.1 | 22.3 | 2450 N–3430 N | 0.26 |

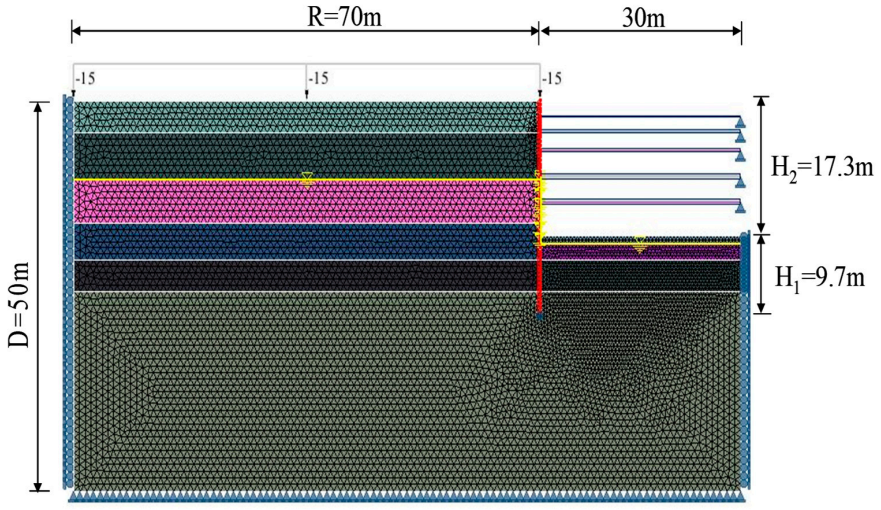


**Figure 18.** SoilWorks simulation analysis model of Case 1.

4.3.1. Description and Input Parameter Selection for Case 3

- Site Description

The site is located at the intersection of Beixin Road Section 3 and Fuxing Road in Xindian District, New Taipei City. It has an irregular shape with an area of approximately 9533 $m^2$ and a height difference of less than 1 m (Chung-Lien Engineering Consultant Corporation, New Taipei City, Taiwan. [50]).

- Subsurface Strata

The subsurface conditions at the site can be divided into four layers from top to bottom (Chung-Lien Engineering Consultant Corporation [50]). A brief description of the general characteristics of each layer is provided, and the simplified engineering parameters for the subsurface layers are shown in Table A13. The groundwater investigation data for the site indicate that the groundwater level is generally around GL.−11 m. For the analysis, the initial groundwater level is set at 11 m below the ground surface.

(1) Fill layer: Consists of yellow-brown sandy clay, silty clay, and silty clay with mud. The thickness is approximately 4.3 m, and the *N*-values range from 1 to 19.
(2) Gravel layer: Contains egg-sized gravel interbedded with yellow-brown silty clay. The thickness is approximately 11 m, and the *N*-values range from 15 to above 50.
(3) Gray sandy clay layer: Consists of gray sandy clay, silty clay, and sandy clay. The thickness is 9.6 m, and the *N*-values range from 7 to 50 (increasing to 50 when encountering gravel). Gravel layer: Contains egg-sized gravel interbedded with yellow-brown silty sand. The thickness is greater than 8.8 m, and the *N*-values are all above 50.

- Foundation Excavation Plan

(1) Geotechnical facilities: The excavation depth is 14.6 m, and the foundation type is a raft foundation. The retaining structure consists of 80 cm thick continuous walls, with a depth of 23.5 m.
(2) Support system: The inverted construction method is adopted for the site, which involves staged excavation and construction of underground floor slabs. The support structures used during the excavation process are 1F, B2FL, and B3FL.
(3) Excavation steps: The excavation is carried out in four stages. In the first stage, the excavation is lowered to GL.−2.5 m to construct the 1F floor slab. In the second stage, the excavation is lowered to GL.−8.0 m to construct the B2F floor slab (GL.−7.025 m). In the third stage, the excavation is lowered to GL.−11.2 m to construct the B3F floor slab (GL.−10.225 m). Finally, in the fourth stage, the excavation is lowered to the final excavation bottom at GL.−14.6 m.

- Determination of Soil and Structural Parameters

Based on the recommended engineering parameters listed in Table A13, the soil input parameters used in the program are shown in Table 12. The retaining walls and floor slabs are simulated using beam elements. The main input data include a cross-sectional area (*A*), Young's modulus (*E*), and the moment of inertia (*I*). The stiffness of the retaining wall is generally reduced by 70% based on empirical experience, while the stiffness of the floor slab is reduced by 25%. The input parameters for the structural elements are shown in Tables 13 and 14.

**Table 12.** Soil strength parameter input table for Case Study 3 in SoilWorks.

| Depth (m) | Soil Classification | Use *N* Value | $c'$ (kN/m$^2$) | $\Phi'$ (°) | $\gamma_{unsat}$ (kN/m$^3$) | $\gamma_{sat}$ (kN/m$^3$) | $E_S$ (kN/m$^2$) | $\nu$ |
|---|---|---|---|---|---|---|---|---|
| 0.0~4.0 | SF, ML, CL | 18 | 0 | 28 | 20.1 | 20.0 | 44,100 N | 0.347 |
| 4.0~15.7 | GW | 44 | 4.9 | 38 | 22.1 | 22.3 | 2450 N–3430 N | 0.263 |
| 15.7~20.3 | ML, SM | 18 | 0 | 31 | 20.0 | 19.3 | 44,100 N | 0.327 |
| 24.4~33.0 | GW | 100 | 9.8 | 40 | 22.1 | 22.3 | 2450 N–3430 N | 0.263 |

**Table 13.** Input parameters for diaphragm wall strength in Case Study 3.

| Thickness (m) | $E$ (kN/m$^2$) | $I$ (m$^4$/m) | Reduction Factor | 0.7$EA$ (kN/m) | 0.7$EI$ (kNm$^2$/m) |
|---|---|---|---|---|---|
| 0.8 | $2.13 \times 10^7$ | 0.04267 | 0.7 | $1.19 \times 10^7$ | $6.36 \times 10^5$ |

**Table 14.** Input parameters for floor structure in Case Study 3.

| Number of Floors | Floor Position | Thickness (cm) | $A$ (m$^2$/m) | 0.25$A$ (m$^2$/m) | $I$ (m$^4$/m) | $E$ (kN/m$^2$) |
|---|---|---|---|---|---|---|
| 1F | GL.+0.0 m | 20 | 0.20 | 0.05 | $6.667 \times 10^{-4}$ | $2.46 \times 10^7$ |
| B2F | GL.−3.9 m | 45 | 0.45 | 0.1125 | $7.594 \times 10^{-3}$ | $2.46 \times 10^7$ |
| B3F | GL.−6.3 m | 45 | 0.45 | 0.1125 | $7.594 \times 10^{-3}$ | $2.46 \times 10^7$ |

- Basic Assumptions

(1) The excavation process is assumed to exhibit plane strain behavior.
(2) Considering the influence range behind the retaining wall, the analysis range (B) extends at least four times the excavation depth beyond the retaining wall. The vertical range (D) is obtained by adding twice the penetration depth (3H1 + H2) to the length of the retaining wall. A uniform distributed load of 15 kN/m$^2$ is assumed to act on the ground surface.
(3) Based on the site conditions, including the excavation depth, shape, support system configuration, and soil layer boundaries, a mesh is created for the analysis. The boundary elements of the mesh are assumed to have no horizontal or lateral displacements outside the influence range.
(4) The stiffness of the retaining wall is reduced by 70% based on empirical experience, while the stiffness of the floor slab is reduced by 25%.
(5) The retaining walls and floor slabs are simulated using beam elements.
(6) The analysis is conducted using 15-node triangular elements.
(7) Based on the observation of previous cases, when the bottom of the retaining wall penetrates the gravel layer to a certain depth (more than 1.5 m below the bottom), no significant horizontal displacements are observed; therefore, in the analysis, horizontal displacements at the bottom of the retaining wall are restricted.

- Analysis Procedure

Considering the monitoring data and construction conditions at the site, the actual excavation steps are simplified for the analysis. Since the B1F floor slab is constructed during the third excavation, its influence on the retaining wall is not considered in the analysis. The groundwater level inside the site is maintained at a depth of 1.0 m below the excavation surface during the excavation process. The construction process for case three is described as follows. The analysis model is shown in Figure 19.

(1) Perform the first-stage excavation to GL.−2.5 m;
(2) Construct the 1FL at GL.−0.0 m;
(3) Perform the second-stage excavation to GL.−8.0 m;
(4) Construct the B2FL at GL.−7.025 m;
(5) Perform the third-stage excavation to GL.−11.2 m;
(6) Construct the B3FL at GL.−10.225 m;
(7) Perform the fourth-stage excavation to GL.−14.6 m (reaching the bottom of the excavation, analysis simulation ends at this point).

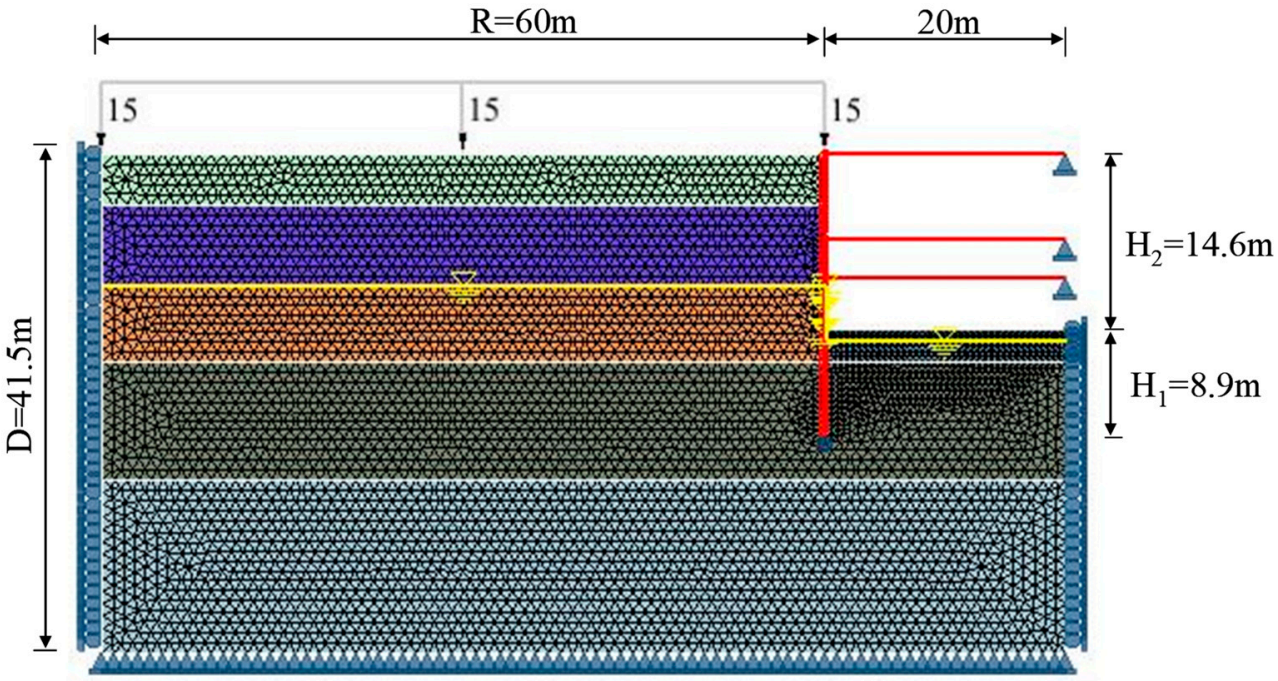


**Figure 19.** SoilWorks simulation analysis model for Case 3.

4.3.2. Feedback Analysis

In this study, a direct method using SoilWorks was employed to simulate the stress–strain behavior of the foundation excavation. The analysis was conducted only for the final excavation stage and compared with the results of Case 1. Since the *N*-values for the second layer (gravel layer) in both cases exceed 50, an *N*-value of 100 was assumed for the analysis. The analysis was performed by varying the soil elastic modulus values incrementally. The analysis results for the final excavation stage in Case 1 and Case 3 using SoilWorks are shown in Figures 20 and 21, respectively.

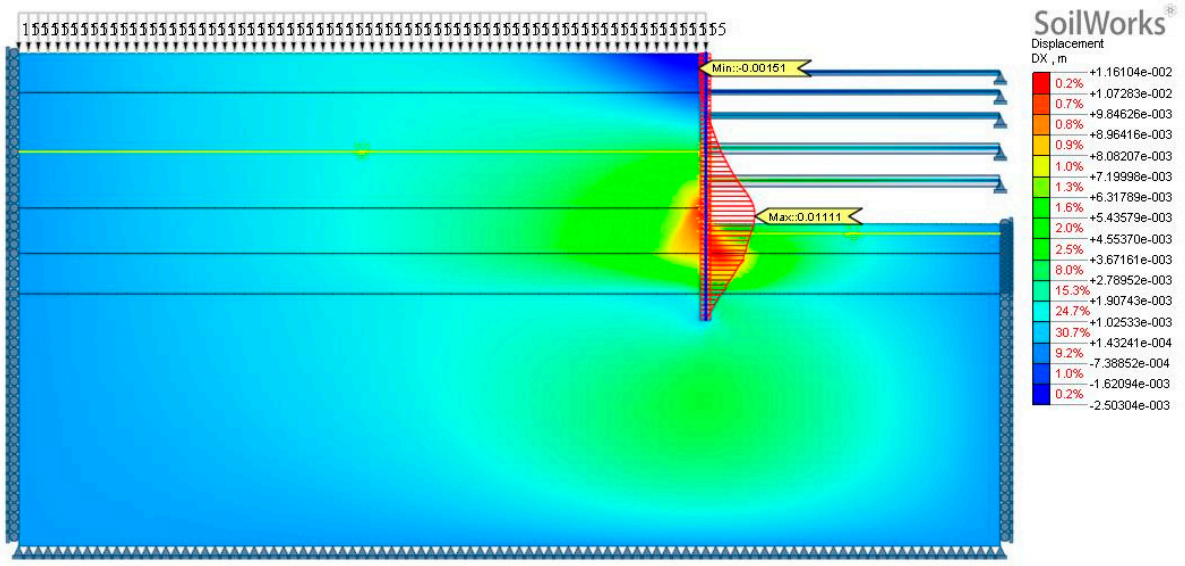


**Figure 20.** Displacement vector diagram of final excavation stage of Case 1 (SoilWorks).

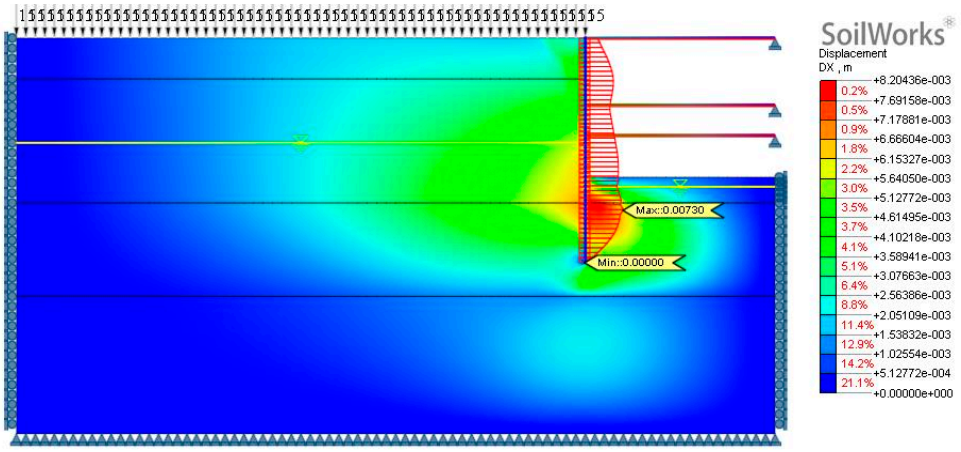


**Figure 21.** Displacement vector diagram of final excavation stage of Case 3 (SoilWorks).

### *4.4. Discussion of Results*

The analysis of the final excavation stage in SoilWorks and the actual deformation curve data of the wall were compared to determine if the wall deformation curve fell within a reasonable estimated range. In this study, a maximum deformation range of ±10% based on actual monitoring data was considered reasonable for both case studies. The results obtained are shown in Figure 22a,b. The following discussion is based on the analysis results:

1. A sensitivity analysis of the effective friction angle in SoilWorks was conducted. The results indicate that *Mmax* and *Dmax* are more sensitive to a smaller friction angle in the sandy and clayey (drained) layers; however, in the clayey (undrained) layer, the sensitivity to the friction angle is lower. Furthermore, comparing the sensitivity analysis results with PLAXIS, it was found that SoilWorks generally exhibits lower sensitivity.
2. A sensitivity analysis of the soil elastic modulus in SoilWorks was conducted. The results show that in both the sandy and clayey (drained and undrained) layers, the elastic modulus values of the soil have a greater influence on *Mmax* and *Dmax*. Comparing the sensitivity analysis results with PLAXIS, it was found that SoilWorks exhibits lower sensitivity than PLAXIS for *Dmax*, while the sensitivities of *Mmax* and *Favg* are comparable between the two.
3. From the sensitivity analysis, it can be concluded that the friction angle and soil elastic modulus are two parameters that have a relatively high sensitivity to the displacement of the retaining wall.
4. Consistent with the previous PLAXIS analysis, when the bottom of the wall reaches a certain depth into rock or gravel layers (more than 1.5 m), there is no horizontal displacement observed at the bottom of the wall; therefore, in the analysis, horizontal displacement at the bottom of the wall was restrained. The analysis results demonstrate consistency with the actual monitoring data in terms of the maximum deformation location and the trend of the wall displacement curve, indicating that this basic assumption in the analysis is reasonable.
5. A feedback analysis was conducted using Case 1, followed by validation using Case 3. The results indicate that under the assumption of $N$ = 100 for the second layer of gravel, within the soil elastic modulus range $2450N$~$3430N$ (kN/m$^2$), a reasonable estimation of the maximum deformation and its occurrence location during the final excavation stage can be achieved under the conditions of gravel layers in the Xindian area.

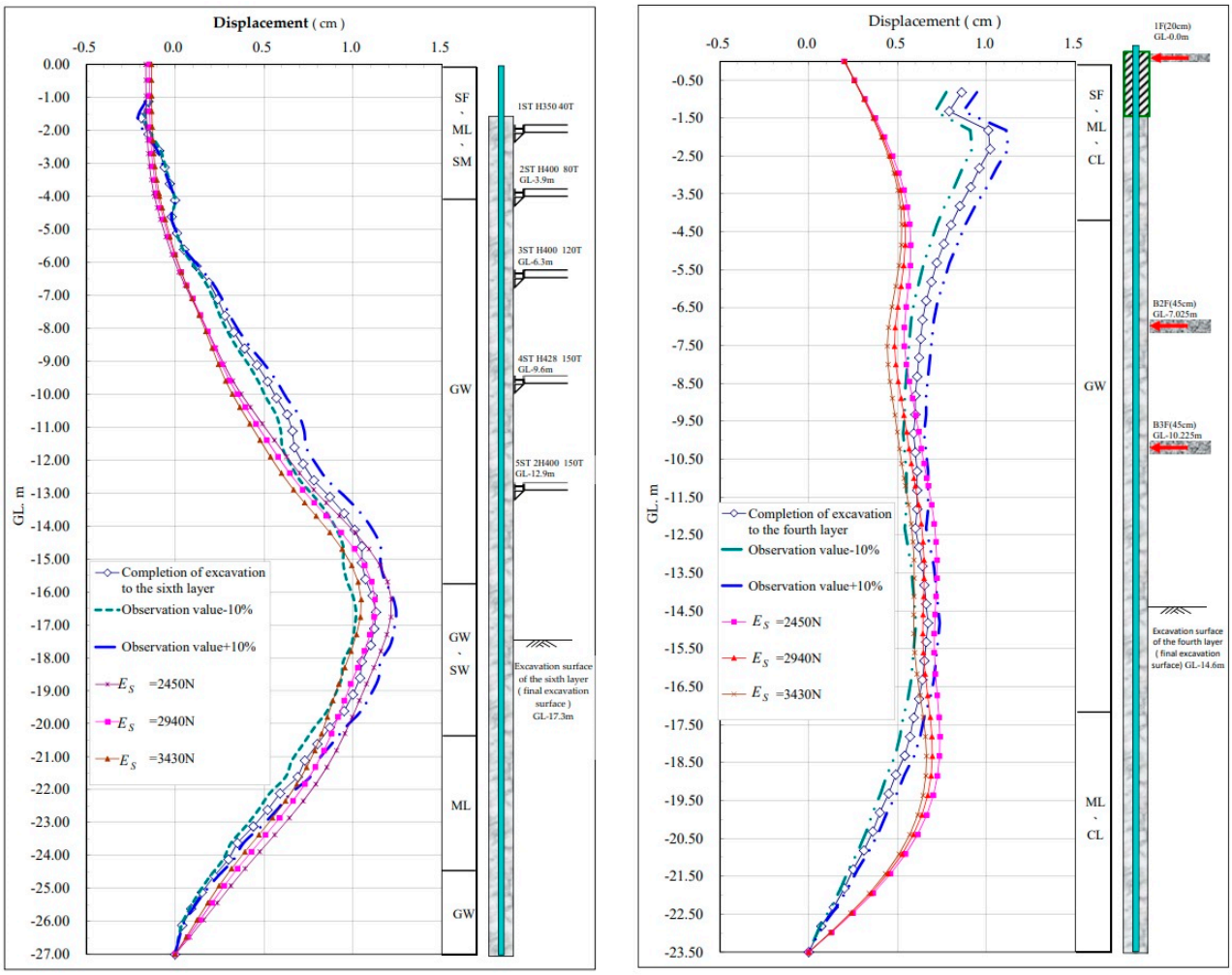


(**a**) (**b**)

**Figure 22.** Comparison diagram of lateral displacement in the final excavation stage of (**a**) Case 1 and (**b**) Case 3 based on SoilWorks model.

## 5. Conclusions

### *5.1. Conclusions*

Based on the research process and findings presented above, the conclusions can be summarized as follows:

- Sensitivity Analysis of Effective Friction Angle in SoilWorks The results indicate that the maximum bending moment and maximum displacement are more sensitive to smaller friction angles in both sandy and clayey (drained) soil layers. In contrast, the sensitivity to the friction angle is lower in the undrained clay layers. Furthermore, upon comparing the sensitivity analysis results with PLAXIS, it was observed that SoilWorks generally exhibits lower sensitivity.
- Sensitivity Analysis of Soil Elastic Modulus in SoilWorks The results show that the maximum bending moment and maximum displacement are more sensitive to changes in soil elastic modulus values, regardless of whether these relate to the sand layer or the clay layer. Comparing the sensitivity analysis results with PLAXIS, it was observed that SoilWorks has lower sensitivity to the maximum displacement but similar sensitivity to the maximum bending moment and average axial force.
- A parameter feedback analysis was conducted for deep excavation using two-dimensional PLAXIS and SoilWorks analysis programs. Based on the feedback analysis results from various practical cases, it was found that for the gravel layer in Xindian area, soil

elastic modulus values of 7840 N/m$^2$; to 9800 N/m$^2$; in PLAXIS and 2450 N/m$^2$; to 3430 N/m$^2$; in SoilWorks can reasonably estimate the maximum deformation in the final excavation stage.

In conclusion, it is recommended that engineers refer to the provided ranges when selecting the soil elastic modulus for excavation analysis in gravel layers in the Xindian area of Taiwan. This will help improve the accuracy of deformation predictions during the final excavation stage. These findings serve as crucial references for engineers and contribute to the effective prediction and management of excavation behavior in civil engineering projects.

### *5.2. Recommendations*

- Based on the sensitivity analysis of the effective friction angle and soil elastic modulus in PLAXIS and SoilWorks, as well as the analysis of three different excavation depths and construction methods, it is evident that the soil elastic modulus has a significant impact on wall displacement. This impact becomes more pronounced with larger excavation scales; therefore, careful evaluation of the input parameters should be exercised during the analysis.
- A parameter feedback analysis was conducted in PLAXIS and SoilWorks exclusively for cases involving gravel layers in the Xindian area. The findings may not be directly applicable to other regions with similar geological conditions. Since gravel layer characteristics can vary across different regions, it is advisable to follow the research process outlined in this study when analyzing specific areas. This approach can provide a broader range of research results for reference to designers and engineers in the future.

**Author Contributions:** Methodology, C.-Y.W. and C.-F.H.; formal analysis, C.-Y.W.; investigation, C.-Y.W.; writing—original draft preparation, C.-Y.W. and C.-F.H.; writing—review and editing, C.-F.H. All authors have read and agreed to the published version of the manuscript.

**Funding:** This research received no external funding.

**Institutional Review Board Statement:** Not applicable.

**Informed Consent Statement:** Not applicable.

**Data Availability Statement:** The data used in this article are not public.

**Conflicts of Interest:** The authors declare no conflict of interest.

## Appendix A

**Table A1.** Suggested table of simplified formation engineering parameters in Case 1.

| Strata Description | $N$ | $\gamma_t$ | Total Stress Effective Stress | | Total Stress Effective Stress | |
|---|---|---|---|---|---|---|
| | | | $C$ | $\Phi$ | $C'$ | $\Phi'$ |
| **The Average Thickness of Each Layer** | **Value** | **kN/m$^3$** | **kN/m$^2$** | **°** | **kN/m$^2$** | **°** |
| 1. The backfill layer gradually becomes yellow-brown with gray clayey silt and silty sand, even with gravel. | 1.5~19 (5) | 19.3 | * 9.8 | * 21 | 0 | 30 |
| Average thickness 4.0 m | | | | | | |
| 2. Yellowish-brown silty coarse, medium, and fine sand mixed with pebbles and gravel | 15~>50 (40) | 21.6 | - | - | * 4.9 | * 38 |
| Average thickness 11.7 m | | | | | | |

**Table A1.** *Cont.*

| Strata Description | $N$ | $\gamma_t$ | Total Stress Effective Stress | | Total Stress Effective Stress | |
|---|---|---|---|---|---|---|
| | | | $C$ | $\Phi$ | $C'$ | $\Phi'$ |
| **The Average Thickness of Each Layer** | **Value** | **kN/m$^3$** | **kN/m$^2$** | **°** | **kN/m$^2$** | **°** |
| 3. Gravel mixed with yellow-brown and gray silty coarse, medium, and fine sand | 20~58 (35) | 21.1 | - | - | * 0 | * 38 |
| Average thickness 4.6 m | | | | | | |
| 4. Gray sandy, clayey silt interbedded with thin sandy soil and clay | 12~26 (16) | 19.4 | 9.8 | 24 | 0 | 32 |
| Average thickness 0.5 m | | | | | | |
| 5. Yellow-brown silty coarse, medium, and fine sand mixed with pebbles and gravel | >50 (100) | * 22.1 | - | - | * 9.8 | * 40 |
| Average thickness 10.0 m (hole bottom) | | | | | | |

Note: "*" indicates estimated values, and "( )" indicates suggested $N$ values. Extracted from the "Geological Survey and Analysis Report of Land Parcels 34 and 110, Dafeng Section, Xindian City, Taipei County" by Chunlian Engineering [28].

**Table A2.** Suggested table of simplified formation engineering parameters in Case 2.

| Strata Description | $N$ | $\gamma_t$ | Total Stress Effective Stress | | Total stress Effective Stress | |
|---|---|---|---|---|---|---|
| | | | $C$ | $\Phi$ | $C'$ | $\Phi'$ |
| **The Average Thickness of Each Layer** | **Value** | **kN/m$^3$** | **kN/m$^2$** | **°** | **kN/m$^2$** | **°** |
| 1. Backfill layer and brownish-yellow clayey silt interbedded with sandy silt | 5~17 (7) | 19.4 | 9.8 | 22 | * 0 | * 30 |
| Average thickness 3.7 m | | | | | | |
| 2. Yellowish-brown silty coarse, medium, and fine sand mixed with pebbles and gravel | 22~>50 (40) | 21.9 | - | - | * 4.9 | * 38 |
| Average thickness 12.4 m | | | | | | |
| 3. Yellow-brown silty soil with coarse, medium, and fine sand and even pebbles mixed with gravel | 16~31 (23) | 21.1 | - | - | * 0 | * 34 |
| Average thickness 3.4 m | | | | | | |
| 4. Gray clayey silt with silty clay and thin layer of fine sand | 11~20 (13) | 19.5 | 9.8 | 24 | 0 | 31 |
| Average thickness 4.9 m | | | | | | |
| 5. Yellow-brown silty coarse, medium, and fine sand mixed with pebbles and gravel | >50 (100) | * 22.1 | - | - | * 9.8 | * 40 |
| Average thickness 11.1 m (hole bottom) | | | | | | |

Note: "*" indicates estimated values, and "( )" indicates suggested $N$ values. Extracted from the "Geological Survey and Analysis Report of Land Parcels 62-1 and Other Seven Parcels, Dafeng Section, Xindian City, Taipei County" by Kenkul Engineering [30].

**Table A3.** Input parameters for diaphragm wall strength.

| Thickness(m) | $E$ (kN/m$^2$) | $I$ (m$^4$/m) | Reduction Factor | 0.7$EA$ (kN/m) | 0.7$EI$ (kNm$^2$/m) |
|---|---|---|---|---|---|
| 0.6 | $2.17 \times 10^7$ | 0.018 | 0.7 | $9.13 \times 10^6$ | $2.739 \times 10^5$ |

Note: $E = 1,500,000 \times \sqrt{f_c\prime}$, $f_c\prime = 210 \mathrm{kg/cm^2}$.

**Table A4.** Input parameters for bracing.

| Number of Supporting Layers | Supporting Position | Model | $A$ (cm$^2$) | 0.5$EA$ (kN) | Preload (kN/m) |
|---|---|---|---|---|---|
| 1ST | GL.−1.5 m | 1 × H 350 | 173.9 | $1.826 \times 10^6$ | 125 |
| 2ST | GL.−4.5 m | 2 × H 350 | 347.7 | $3.651 \times 10^6$ | 200 |
| 3ST | GL.−8.0 m | 2 × H 400 | 437.4 | $4.592 \times 10^6$ | 300 |

**Table A5.** Input parameters for soil parameters of sandy layers.

| Depth (m) | Soil Classification | $C'$ (kN/m$^2$) | $\Phi'$(°) | $\gamma_{unsat}$(kN/m$^3$) | $\gamma_{sat}$(kN/m$^3$) | $Es$ (kN/m$^2$) | υ |
|---|---|---|---|---|---|---|---|
| 10 | SM | 1 | 30 | 20 | 21 | 12,500 | 0.32 |
| 20 | SM | 1 | 30 | 20 | 21 | 37,500 | 0.32 |
| 30 | SM | 1 | 30 | 20 | 21 | 62,500 | 0.32 |
| 40 | SM | 1 | 30 | 20 | 21 | 87,500 | 0.32 |
| 42 | SM | 1 | 30 | 20 | 21 | 812,500 | 0.32 |

**Table A6.** Input parameters for soil parameters of clay layers.

| Depth (m) | Soil Classification | $C'$ (kN/m$^2$) | $\Phi'$(°) | $\gamma_{unsat}$(kN/m$^3$) | $\gamma_{sat}$(kN/m$^3$) | $Es$(kN/m$^2$) | υ |
|---|---|---|---|---|---|---|---|
| 10 | CL | 5 | 20 | 19 | 18 | 10,000 | 0.35 |
| 20 | CL | 5 | 23 | 19 | 18 | 18,750 | 0.35 |
| 30 | CL | 5 | 25 | 19 | 18 | 31,250 | 0.35 |
| 40 | CL | 5 | 28 | 19 | 18 | 43,750 | 0.35 |
| 42 | CL | 5 | 30 | 19 | 18 | 56,250 | 0.35 |

**Table A7.** Sensitivity analysis results of elastic modulus for sandy layers.

| SM | *Mmax* | Percentage Change | *Dmax* | Percentage Change | *Favg* | Percentage Change |
|---|---|---|---|---|---|---|
| | (kN-m) | (%) | (mm) | (%) | (kN/m) | (%) |
| 0.5E | 371.32 | 115% | 48.483 | 147% | 246.1 | 100% |
| 0.75E | 342.43 | 106% | 38.368 | 117% | 244.9 | 100% |
| 1.0E | 323.07 | 100% | 32.872 | 100% | 245.4 | 100% |
| 1.5E | 297.63 | 92% | 27.075 | 82% | 248.2 | 101% |
| 2.0E | 280.69 | 87% | 23.941 | 73% | 251.7 | 103% |

**Table A8.** Sensitivity of elastic modulus for sandy layers in PLAXIS and SoilWorks.

| SM | *Mmax* Percentage Change | | *Dmax* Percentage Change | | *Favg* Percentage Change | |
|---|---|---|---|---|---|---|
| | Siolworks | PLAXIS | Siolworks | PLAXIS | Siolworks | PLAXIS |
| 0.5E | 115% | 123% | 147% | 176% | 100% | 103% |
| 0.75E | 106% | 108% | 117% | 125% | 100% | 101% |
| 1.0E | 100% | 100% | 100% | 100% | 100% | 100% |
| 1.5E | 92% | 90% | 82% | 73% | 101% | 99% |
| 2.0E | 87% | 83% | 73% | 59% | 103% | 98% |

**Table A9.** Sensitivity analysis results of elastic modulus for clay layers (undrained).

| CL (Undrained) | *Mmax* | Percentage Change | *Dmax* | Percentage Change | *Favg* | Percentage Change |
|---|---|---|---|---|---|---|
| | (kN-m) | (%) | (mm) | (%) | (kN/m) | (%) |
| 0.5E | 327.72 | 130% | 81.231 | 173% | 257.0 | 106% |
| 0.75E | 279.50 | 111% | 58.627 | 125% | 247.5 | 103% |
| 1.0E | 251.72 | 100% | 46.867 | 100% | 241.4 | 100% |
| 1.5E | 221.83 | 88% | 34.688 | 74% | 234.4 | 97% |
| 2.0E | 205.65 | 82% | 28.341 | 60% | 231.2 | 96% |

**Table A10.** Sensitivity of elastic modulus for clay layers (undrained) in PLAXIS and SoilWorks.

| CL (Undrained) | *Mmax* Percentage Change | | *Dmax* Percentage Change | | *Favg* Percentage Change | |
|---|---|---|---|---|---|---|
| | Siolworks | PLAXIS | Siolworks | PLAXIS | Siolworks | PLAXIS |
| 0.5E | 130% | 135% | 173% | 185% | 106% | 106% |
| 0.75E | 111% | 113% | 125% | 129% | 103% | 102% |
| 1.0E | 100% | 100% | 100% | 100% | 100% | 100% |
| 1.5E | 88% | 85% | 74% | 70% | 97% | 98% |
| 2.0E | 82% | 76% | 60% | 55% | 96% | 96% |

**Table A11.** Sensitivity analysis results of elastic modulus for clay layers (drained).

| CL (Drained) | *Mmax* | Percentage Change | *Dmax* | Percentage Change | *Favg* | Percentage Change |
|---|---|---|---|---|---|---|
| | (kN-m) | (%) | (mm) | (%) | (kN/m) | (%) |
| 0.5E | 439.21 | 116% | 71.259 | 152% | 260.5 | 102% |
| 0.75E | 403.60 | 107% | 55.556 | 119% | 256.3 | 100% |
| 1.0E | 377.30 | 100% | 46.818 | 100% | 255.4 | 100% |
| 1.5E | 348.20 | 92% | 37.725 | 81% | 253.6 | 99% |
| 2.0E | 327.66 | 87% | 32.639 | 70% | 254.3 | 100% |

**Table A12.** Sensitivity of elastic modulus for clay layers (drained) in PLAXIS and SoilWorks.

| CL (Drained) | *Mmax* Percentage Change | | *Dmax* Percentage Change | | *Favg* Percentage Change | |
|---|---|---|---|---|---|---|
| | Siolworks | PLAXIS | Siolworks | PLAXIS | Siolworks | PLAXIS |
| 0.5E | 116% | 124% | 152% | 173% | 102% | 104% |
| 0.75E | 107% | 108% | 119% | 125% | 100% | 101% |
| 1.0E | 100% | 100% | 100% | 100% | 100% | 100% |
| 1.5E | 92% | 89% | 81% | 74% | 99% | 99% |
| 2.0E | 87% | 82% | 70% | 61% | 100% | 98% |

**Table A13.** Recommended simplified geotechnical parameters for Case Study 3.

| Strata Description | | *N* | $\gamma_t$ | Total Stress Effective Stress | | Total Stress Effective Stress | |
|---|---|---|---|---|---|---|---|
| | | | | *C* | $\Phi$ | $C'$ | $\Phi'$ |
| Bottom Depth of Each Layer | | Value | kN/m$^3$ | kN/m$^2$ | ° | kN/m$^2$ | ° |
| 1. | The backfill layer gradually becomes yellow-brown sandy, clayey sediment and muddy clay | 1~19 | 20.1 | 9.8 | 24 | 0 | 28 |
| Average thicknes 4.3 m | | | | | | | |

**Table A13.** *Cont.*

| Strata Description | $N$ | $\gamma_t$ | Total Stress Effective Stress | | Total Stress Effective Stress | |
|---|---|---|---|---|---|---|
| | | | $C$ | $\Phi$ | $C'$ | $\Phi'$ |
| **Bottom Depth of Each Layer** | **Value** | **kN/m$^3$** | **kN/m$^2$** | **°** | **kN/m$^2$** | **°** |
| 2. Pebble gravel with yellowish-brown argillaceous sand | 15~>50 | 22.1 | - | - | * 4.9 | * 38 |
| Average thicknes 13.0 m | | | | | | |
| 3. Gray sandy, clayey mud and muddy sand | 7~50 | 20.0 | 4.9 | 26 | 0 | 31 |
| Average thicknes 9.8 m | | | | | | |
| 4. Pebble gravel, with yellowish-brown argillaceous sand | >50 | * 22.1 | - | - | * 9.8 | * 40 |
| Average thicknes 11.1 m (hole bottom) | | | | | | |

Note: "*" indicates estimated values. Extracted from the "Geological Survey and Analysis Report of Land Parcels 21, 22, 22-1, 24, 24-1, 26, 26-1, 69, and 79, Fuxing Section, Xindian City, Taipei County" by Chunlian Engineering [34].

## Appendix B

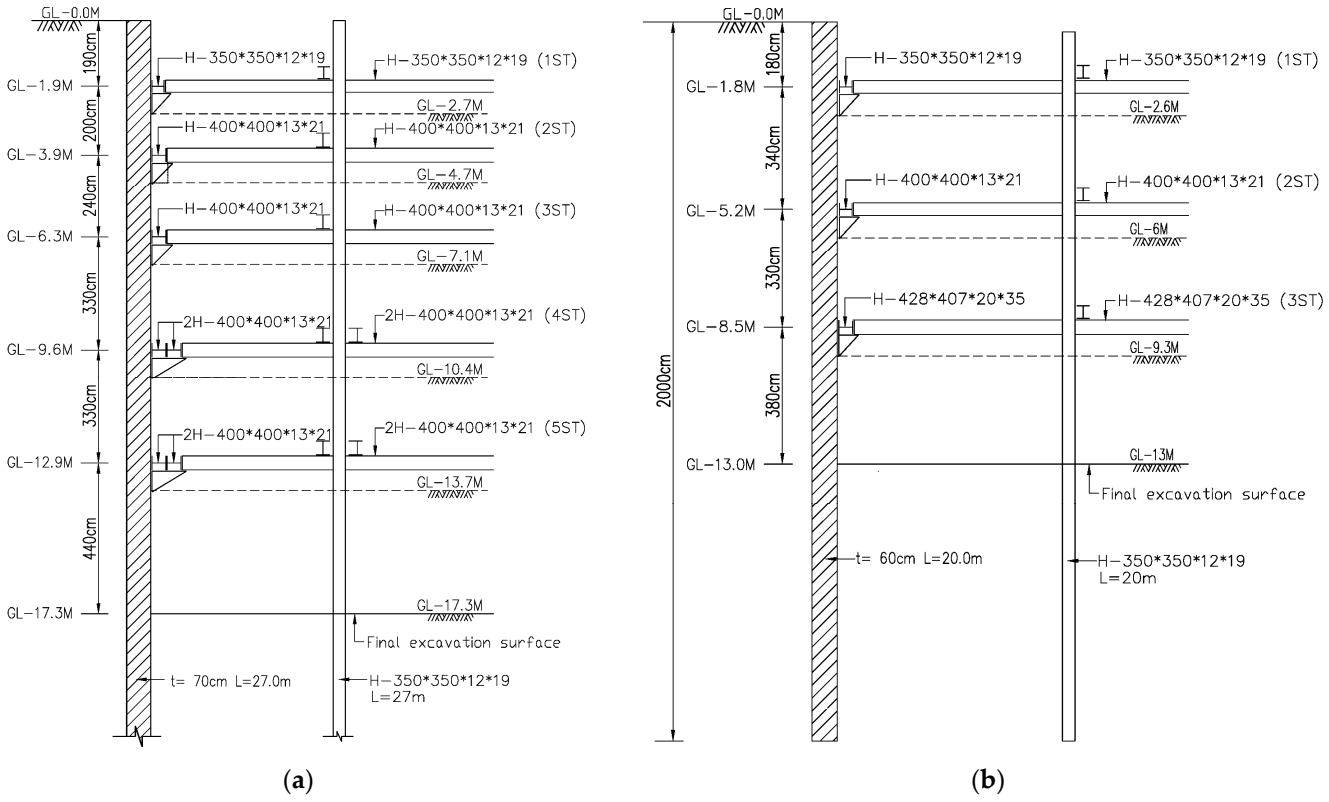


**Figure A1.** Sectional view of excavation support in (**a**) Case 1 and (**b**) Case 2.

## References


1. Hong, R.J. *Comprehensive Investigation and Study of Underground Geology and Engineering Environment in Taipei Basin: Research on Stratigraphic Distribution*; Central Geological Survey Report; Report No. 83-009; Central Geological Survey, MOEA: New Taipei, Taiwan, 1994.
2. Liu, Z.L. Seismic Microzonation Map of Taipei Basin. Master's Thesis, National Central University, Taoyuan, Taiwan, 1994.
3. Li, X.H. Engineering Geological Zoning of Taipei City. *Geotech. Technol.* **1996**, 25–34. [CrossRef]
4. PLAXIS BV. *Plaxis Version 8 Manual*; Delft University of Technology & PLAXIS b.v.: Amsterdam, The Netherlands, 2006.
5. Huang, C.Y. Application of Neural Networks in Predicting Deformation of Deep Excavation Walls. Master's Thesis, National Taiwan Ocean University, Keelung, Taiwan, 2002.
6. Chen, J.Q.; Ji, S.Y. *Study on Characteristics and Deep Excavation Behavior of Soft Soil Layers (I): Research on Analysis Program for Interaction between Deep Excavation Soil and Support*; Chunghsing Engineering Consulting Corporation: Taipei, Taiwan, 1996.
7. Ji, S.Y.; Chen, J.Q. Numerical Simulation of Time-Dependent Deep Excavation Construction. In Proceedings of the 7th Geotechnical Engineering Conference, Hsinchu, Taiwan, 11–15 June 1997; pp. 609–615.
8. Tang, Y.G. Study on Soil Parameter Identification for Deep Excavation Analysis. Ph.D. Dissertation, National Taiwan University of Science and Technology, Taipei, Taiwan, 1998.
9. Xie, B.G.; Ou, Z.Y. Deep Excavation Analysis under Undrained Conditions Using a Pseudo-Plastic Model. *J. China Civ. Eng.* **2000**, *12*, 703–713.
10. He, Z.D. Deep Excavation Analysis in Soft Soil Layers. Master's Thesis, National Taipei University of Technology, Taipei, Taiwan, 2004.
11. Chen, C.G. Preliminary Study on Simulating the Behavior of Excavation and Support using RIDO and PLAXIS Programs. Master's Thesis, National Ilan University, Yilan, Taiwan, 2011.
12. Wang, K.; Li, W.; Sun, H.; Pan, X.; Diao, H.; Hu, B. Lateral Deformation Characteristics and Control Methods of Foundation Pits Subjected to Asymmetric Loads. *Symmetry* **2021**, *13*, 476. [CrossRef]
13. Yazici, M.F.; Keskin, S.N. Optimum Design of Multi-anchored Larssen Type Sheet Pile Wall for Temporary Construction Works. *Geomech. Eng.* **2021**, *27*, 1–11. [CrossRef]
14. Hong, L.; Chen, L.; Wang, X. Reliability Analysis of Serviceability Limit State for Braced Excavation Considering Multiple Failure Modes in Spatially Variable Soil. *Buildings* **2022**, *12*, 722. [CrossRef]
15. Nguyen, B.P.; Ngo, C.P.; Tran, T.D.; Bui, X.C.; Doan, N.-P. Finite Element Analysis of Deformation Behavior of Deep Excavation Retained by Diagram Wall in Ho Chi Minh City. *Indian Geotech. J.* **2022**, *52*, 989–999. [CrossRef]
16. Rahmani, F.; Hosseini, S.M.; Khezri, A.; Maleki, M. Effect of grid-form deep soil mixing on the liquefaction-induced foundation settlement, using numerical approach. *Arab. J. Geosci.* **2022**, *15*, 1112. [CrossRef]
17. Maleki, M.; Imani, M. Active lateral pressure to rigid retaining walls in the presence of an adjacent rock mass. *Arab. J. Geosci.* **2022**, *15*, 152. [CrossRef]
18. Maleki, M.; Mir Mohammad Hosseini, S. Seismic Performance of Deep Excavations Restrained by Anchorage System Using Quasi Static Approach. *J. Seismol. Earthq. Eng.* **2019**, *21*, 11–21. [CrossRef]
19. Bjerrum, L. *Observed versus Computed Settlement of Structures on Clay and Sand*; Massachusetts Institute of Technology: Cambridge, MA, USA, 1964.
20. D'Appolonia, D.J. Settlement of Spread Footing and Design. *J. Soil Mech. Found. Div.* **1970**, *94*, SM3.
21. Shimons, N.E.; Menzies, B.K. *A Short Course in Foundation Engineering*; Butterworth & Co., Ltd.: London, UK, 1977.
22. Bowles, J.E. *Foundation Analysis and Design*, 3rd ed.; Mc Graw-Hill: New York, NY, USA, 1982; pp. 1159–1177.
23. Li, W.F.; Lai, Y.R.; Liao, N.H. Two-Dimensional Numerical Analysis Method for Soil Nailing Reinforced Slopes. *Geotech. Technol.* **2003**, *98*, 39–54.
24. Hsieh, H.S.; Cheng, J.S.; Tsai, Z.H.; Yang, M.C. Practical Considerations for Continuous Wall Design Analysis. *Geotech. Technol.* **1996**, *53*, 35–44.
25. Zhang, J.Z.; Chen, K.Q. Assessment of Sensitivity of Design Parameters on Deep Excavation and Retaining Wall. *Geotech. Technol.* **1999**, *76*, 17–24. [CrossRef]
26. Qiu, Z.R. Study on Parameters of Deep Excavation in Sanchong-Luzhou Area. Master's Thesis, National Taipei University of Technology, Taipei, Taiwan, 2007. [CrossRef]
27. Hong, Z.S.; Zeng, L.L.; Cui, Y.J.; Cai, Y.Q.; Lin, C. Compression behaviour of natural and reconstituted clays. *Géotechnique* **2012**, *62*, 291–301. [CrossRef]
28. Yao, Y.-P.; Hou, W.; Zhou, A.-N. UH model: Three-dimensional unified hardening model for over-consolidated clays. *Géotechnique* **2009**, *59*, 451–469. [CrossRef]
29. Yao, Y.P.; Zhou, A.N. Non-isothermal unified hardening model: A thermo-elastoplastic model for clays. *Géotechnique* **2013**, *63*, 1328–1345. [CrossRef]
30. Clough, G.W.; O'Rourke, T.D. Construction Induced Movements of In-Situ Walls. In *Design and Performance of Earth Retaining Structures (GSP 25)*; ASCE: Reston, VA, USA, 1990; pp. 154–196.
31. Jin, Y.F.; Yin, Z.Y.; Shen, S.L.; Hicher, P.Y. Selection of sand models and identification of parameters using an enhanced genetic algorithm. *Int. J. Numer. Anal. Methods Geomech.* **2016**, *40*, 1219–1240. [CrossRef]

32. Cui, Q.-L.; Shen, S.-L.; Xu, Y.-S.; Wu, H.-N.; Yin, Z.-Y. Mitigation of Geohazards during Deep Excavations in Karst Regions with Caverns: A Case Study. *Eng. Geol.* **2015**, *195*, 16–27. [CrossRef]
33. Elbaz, K.; Shen, S.L.; Cheng, W.C.; Arulrajah, A. Cutter-Disc Consumption during Earth Pressure Balance Tunnelling in Mixed Strata. *Geotech. Eng.* **2018**, *171*, 363–376. [CrossRef]
34. Midas Co., Ltd. *SoilWorks Program User Manual*; Midas Co., Ltd.: New Taipei City, Taiwan, 2012.
35. Hong, R.J. Preliminary Study on Composite Soil Engineering Properties. *J. Eng. Natl. Taiwan Univ.* **1978**, *23*, 1–12.
36. Das, B. *Fundamentals of Geotechnical Engineering*, 3rd ed.; PWS: Boston, MA, USA, 1994; pp. 81–82.
37. Ou, C.Y. *Design Theory and Practice of Deep Excavation Method Analysis*; Technology Press Co., Ltd.: Taipei City, Taiwan, 2002.
38. Chuung, C.h. Investigation of the Influence of Mesh Boundaries on Finite Element Excavation Analysis Results. Master's Thesis, National Taiwan University of Science and Technology, New Taipei, Taiwan, 2008.
39. Maleki, M.; Khezri, A.; Nosrati, M.; Hosseini, S.M.M.M. Seismic amplification factor and dynamic response of soil-nailed walls. *Model. Earth Syst. Environ.* **2023**, *9*, 1181–1198. [CrossRef]
40. Maleki, M.; Nabizadeh, A. Seismic performance of deep excavation restrained by guardian truss structures system using quasi-static approach. *SN Appl. Sci.* **2021**, *3*, 417. [CrossRef]
41. Maleki, M.; Mir Mohammad Hosseini, S.M. Assessment of the Pseudo-static seismic behavior in the soil nail walls using numerical analysis. *Innov. Infrastruct. Solut.* **2022**, *7*, 262. [CrossRef]
42. Kenkul Engineering Co., Ltd. *Completion Report of Foundation Construction Safety Observation for Jianglinchun Phase 1 Building Project 2005a*; Kenkul Engineering Co., Ltd.: New Taipei City, Taiwan, 2005.
43. Lin, C.M. Numerical Simulation of Excavation in Gravel Layers. Master's Thesis, National Taiwan Ocean University, Keelung, Taiwan, 2011.
44. Chunglian Engineering Consultants Co., Ltd. *Geological Investigation and Analysis Report for Land Parcels 34 and 110, Dafeng Section, Xindian City, Taipei County*; Chunglian Engineering Consultants Co., Ltd.: New Taipei City, Taiwan, 2003.
45. Kenkul Engineering Co., Ltd. *Completion Report of Foundation Construction Safety Observation for Jianglinchun Phase 2 Building Project*; Kenkul Engineering Co., Ltd.: New Taipei City, Taiwan, 2006.
46. Kenkul Engineering Co., Ltd. *Geological Investigation and Analysis Report for Land Parcels 62-1 and Seven Others, Dafeng Section, Xindian City, Taipei County, 2005b*; Kenkul Engineering Co., Ltd.: New Taipei City, Taiwan, 2005.
47. Fan, C.Y. Finite Element Analysis of Mutual Effects of Adjacent Excavation Sites. Master's Thesis, Feng Chia University, Taichung, Taiwan, 2005.
48. Guo, T.Y. Numerical Analysis Study of Deformation Behavior in Gravel Layer Tunnels. Master's Thesis, National Cheng Kung University, Tainan, Taiwan, 1999.
49. Hou, Z.A. Feedback Analysis of Excavation Procedure and Optimal Support Types in Cobble Gravel Layers. Master's Thesis, National Chung Hsing University, Taichung, Taiwan, 2001.
50. Chunglian Engineering Consultants Co., Ltd. *Geological Investigation and Analysis Report for Land Lots with Nine Parcel Numbers, Section 21, 22, 22–1, 24, 24-1, 26, 26–1, 69, and 79, Xindian District, Taipei County, 2006*; Chunglian Engineering Consultants Co., Ltd.: New Taipei City, Taiwan, 2006.